Exploration of Various Aspects of UGA-SUMRCC: Size Extensivity, Possible Use of Sufficiency Conditions, and an Extension for Direct Determination of Energy Differences

Avijit Shee, Sangita Sen, Debashis Mukherjee

Exploration of Various Aspects of UGA-SUMRCC: Size Extensivity, Possible Use of Sufficiency Conditions, and an Extension for Direct Determination of Energy Differences

Avijit Shee,[†,‡] Sangita Sen,[†] and Debashis Mukherjee*[,†]

[†]Raman Center for Atomic, Molecular and Optical Sciences, Indian Association for the Cultivation of Science, Kolkata 700 032, India

[‡]Laboratoire de Chimie et Physique Quantique (UMR 5626), CNRS/Université de Toulouse 3 (Paul Sabatier), 118 route de Narbonne, 31062 Toulouse, France

ABSTRACT: The Unitary Group Adapted State Universal Multireference Coupled Cluster (UGA-SUMRCC) theory, recently developed by us (J. Chem. Phys. 2012, 137, 074104), contains exactly the right number of linearly independent cluster operators. This avoids any redundancy of the excitation manifold in a way exactly paralleling the traditional spin− orbital based SUMRCC. The choice of the linearly in-dependent cluster operators inducing the same change of orbital occupancy becomes increasingly cumbersome if we go over to the cases of active CSFs with more than two active quasiparticles. In the present development, we explore several aspects of the UGA-SUMRCC theory: (a) The first is a variant where we have deliberately incorporated redundancy of the cluster amplitudes to simplify the working equations and have shown that it can serve as a very good approximation to the parent UGA-SUMRCC theory for states with more than two valence occupancies. This in turn suggests that it could be a useful avenue to pursue for arbitrary mh−np situation since the working equations assume simpler algebraic structure in such cases. (b) The analyses of the aspects of size extensivity are known to involve greater complexity if they involve various reduced density matrices (RDMs), since the RDMs are not size-extensive quantities. We have presented the proof for UGA-SUMRCC starting from equations containing h−p RDMs via a decomposition involving products of size-extensive cumulants and argue that it has relevance for general cases beyond the h−p model spaces. (c) A useful extension of UGA-SUMRCC lies in formulating the theory for direct calculations of energy differences of spectroscopic interest such as excitation energies, ionization potentials, and electron affinities relative to a closed shell ground state, thus providing attractive alternatives to other allied methods such as SAC-CI, CC-LRT, EOM-CC, STEOM-CC, or ADC. This extension, called UGA-based Quasi-Fock MRCC by us, also leads to exact cancellation of common correlation terms between the initial and final states. Taking a cue from the hierarchical development in Fock-space theories but keeping in mind the advantages of a state-universal (equivalently called a valence specific) theory, our formulation proposes a spin-adapted, accurate, and compact scheme for studying such energy differences. Our results demonstrate superior performance of the method as compared to EOM-CC.

1. INTRODUCTION

Coupled cluster theory[1−5] has emerged as by far the most reliable method for energy and properties of molecular electronic states dominated by a single reference function. For states involving quasi-degeneracy, the behavior of the so-called "gold standard" single reference coupled cluster (SRCC), viz. the CCSD(T),[6] becomes erratic, although more involved approaches have been suggested within the framework of SRCC but invoking higher level approximations.[7,8] Multireference Coupled Cluster (MRCC) theories seem like a more natural choice to handle such situations, and the past three decades have seen considerable developments along several avenues. Despite the undeniable success of several methodologies, the black box use of MRCC theories is still difficult. One major challenge for treating open shell and multireference states (whether at the single or at the multireference level) is the spin adaptation of the coupled cluster wave function. For single determinant nonsinglet states, one usually adopts a spin−orbital based theory to achieve a natural termination at the quartic level and it is well-known that this leads to spin-broken solutions.[9] At the MRCC level, the degree of difficulty of spin adaptation depends on the class of MRCC theory one wants to adapt to the proper spin. It is also well documented that spin adaptation has a small but significant role in the accuracy of state energies and that it plays a vital role in the computed properties of molecules. Among the three major approaches to MRCC, viz., valence universal or Fock-Space (VUMRCC or FS-MRCC),[10−13] state universal (SUMRCC),[14,15] and state specific (SSMRCC),[16] only the VUMRCC is inherently spin

adapted. It is also a natural theory for direct computation of energy differences. On the other hand, the Jeziorski–Monkhorst (JM) Ansatz[14] used in the last two types of MRCC theories is not inherently spin adapted and in a truncated coupled-cluster scheme results in spin broken solutions for non-singlet states. The spin adaptation of the JM Ansatz has been the subject of much research.[17−23] The most recent endeavor in this direction has been the use of the normal ordered JM-like Ansatz with cluster operators defined in terms of unitary generators, first introduced by Maitra et al.[22] This Ansatz was first applied by Maitra et al.[22] in the context of SS-MRCC. The model functions in this approach are Unitary Group Adapted (UGA) Gel'fand states, and to indicate this the method was termed a Unitary Group Adapted SSMRCC (UGA-SSMRCC) theory. It combines the twin advantages of the avoidance of spin contamination and a natural termination of the so-called "direct" term at the quartic power of the working equations of the SSMRCC theory. Following an early lead by Mukherjee and Zaitseveskii,[24] we were led to the same Ansatz to formulate an UGA-SUMRCC[23] theory which also shares the desirable properties of the absence of spin contamination as well as termination of the direct term at the quartic power. We should mention here that another spin-free generalization of the JM Ansatz, using unitary generators, was suggested by Datta and Mukherjee, which is known as COS-SUMRCC[20] and COS-SSMRCC.[21] They are structurally closer to the parent spin–orbital based JM Ansatz and are thus probably the closest spin-free analogue of JM based MRCC theories. The acronym "COS" signifies a "combinatoric open-shell" situation where the combinatoric factor accompanying the nth power of the cluster operator is taken to be the inverse of the "automorphic factor." The applications thereof are still confined to one valence problem, although generalization to encompass multivalence situations is expected to indicate the potentiality of the approach. As things are at present, the UGA-based SU- and SS-MRCC[22,23] appear to be simpler—though admittedly somewhat less rich—alternatives. The preliminary applications indicate the potentiality of both the SU- and SS- methods and thus warrant further explorations. We propose to address in this paper various important aspects of the UGA-SUMRCC. The excursions covered by us in this paper will be delineated as we go along.

Unlike in the SSMRCC theory and its UGA version, where the number of cluster amplitudes exceeds the number of virtual functions—thus requiring the use of suitable sufficiency conditions to resolve the redundancy—there are no redundant cluster amplitudes in the parent spin–orbital-based SUMRCC. While formulating the UGA-SUMRCC, it would be natural to include only those cluster operators for the various T_μ's which lead to just the right number of virtual functions χ^l_μ by their action on model configuration state functions (CSFs), ϕ_μ. This was the strategy adopted by us in our recent UGA-SUMRCC formulation.[23] Using the singles and doubles (SD) truncation scheme, not all the virtual functions χ^l_μ generated by single and double orbital substitutions are reachable using one and two body unitary generators accompanying the cluster operators in T_μ in the general situation (i.e., arbitrary valence occupancy in ϕ_μ's). The χ^l_μs thus span a subset of linearly independent virtual functions, which depends on both the spin-multiplicity and the number of active orbitals in ϕ_μ. In addition to having an incomplete spanning of the space of virtual functions via singles and doubles in T_μ, some virtual functions reached can even be linearly dependent. The latter is more frequent when the number of active orbitals is rather few. There are two ways to choose the cluster operators in such a situation: (a) use suitable combinations of unitary generators to define the linearly independent combination of excitation operators and (b) continue to use the simple unitary generators, and in case their number exceeds the number of linearly independent excitations one includes redundant operators and provides extra working equations by invoking sufficiency conditions. Approach b is entirely conceivable and natural for UGA-SSMRCC, since one is obliged to invoke sufficiency conditions anyway. Such a strategy was indeed adopted by Maitra et al.[22] in their UGA-SSMRCC and a related theory where the inactive double excitations were treated in an internally contracted manner (UGA-ICID-SSMRCC).[25] In the realm of UGA-SUMRCC, such sufficiency conditions do not appear, but it is not mandatory to disallow redundancy such as has been employed in the UGA-SSMRCC. The use of redundant cluster operators may lead to simpler working equations whose efficacy needs to be looked into. In our first formulation,[23] we have applied the theory for state energies *per se* of the cationic, anionic, and excited states. With our choice of vacuum as the Hartree–Fock function, it is worth looking into the possibility of a formulation for excitation energy directly in a spin-free manner. In this paper, we will explore the efficacy and utility of three distinct modifications:

(i) The first issue, that we will consider, pertains to analyzing our choice of cluster operators vis-a-vis those used by Li and Paldus[17] to formulate SUMRCC in a UGA framework. In particular, we will show that suitable linearly independent cluster operators can be discerned from simple perturbative reasoning, although they will no longer lead to orthogonal excited functions. In effect, for the singles–doubles truncation scheme our choice of combinations appears to be the same as that obtained from explicit SU2 adaptation.[17] We shall demonstrate that, if we include some redundant cluster operators, it is possible to generate a set of spin-free UGA-SUMRCC equations for excited state energies and excitation energies which are of the same structure irrespective of spin multiplicity. One avenue which we shall look into is the possibility of deliberately using certain redundant cluster operators and concomitantly using suitable sufficiency conditions to generate the working equations.

(ii) We shall also try to assess the relative importance of the inclusion of higher body connected composites in the modified UGA-SUMRCC equation. Since we have already looked into the effect of such higher body blocks in the parent UGA-SUMRCC theory,[23] we think that it is worthwhile to look at the importance of the higher body contribution in the modified theory also.

(iii) The third issue we will look into is to transcribe the UGA-SUMRCC theory for state energies to a theory for computing energy differences directly with respect to the ground state. The Fock space MRCC (FS-MRCC) theory, also known as the Valence Universal Multi-Reference Coupled Cluster Theory (VUMRCC), achieves this by carrying out computations on all subduced valence sectors leading up to the target valence sector.[13] Our efforts are directed toward the formulation of a theory for calculating the direct energy difference for the target sector with respect to the ground state *without going through intermediate valence sectors*. Thus, in our strategy, the computation of excitation energy does not involve a prior computation of ionization energy and electron affinity and the associated cluster amplitudes. We call this formulation a unitary group adapted Quasi-Fock multireference coupled cluster (UGA-QFMRCC) theory.

In this paper, we will also discuss in detail several aspects of connectivity and size extensivity of the parent UGA-SUMRCC

and the consequent size intensivity of the excitation energies from UGA-QFMRCC. A general guideline for proving the connectedness of such UGA-MRCC theories is presented, which can be extended to any valence sector and rank of operator, although the consequent derivations become increasingly more involved with the increase in either valence or operator rank.

A study of the performance of all our proposed variants across a chosen set of small molecules is undertaken. We have assessed the trends in energies computed using UGA-SUMRCC and its approximants along a series of basis sets of increasing quality. Statistical data in a reasonable sample space is provided for a more objective analysis.

This paper is organized as follows: In section 2, section 2.1 presents a summary of the development of the UGA-SUMRCC theory, while section 2.2 describes the Ansatz for direct calculation of energy differences and the derivation of the working equations therein. In section 3, the choice of cluster operators in a spin-free UGA-SUMRCC or UGA-QFMRCC is discussed. Section 3.1 demonstrates the rigorous choices we could make and 3.2 deals with certain approximations in the form of sufficiency conditions which could be invoked to simplify the equations. Section 3.3 contains a discussion about the physical content of UGA-QFMRCC, in comparison to other existing methodologies for direct computation of excitation energies. In section 4, a general proof of size extensivity for the parent UGA-SUMRCC and UGA-QFMRCC is delineated. In section 5.1, we discuss the aspects of computational organization and in section 5.2 the computational cost of UGA-QFMRCC. In section 5.3, we present our results and explore the performance of the variant using sufficiency against the parent UGA-SUMRCC and the Quasi-Fock theory against the parent UGA-SUMRCC theory. We also compare our results with those from related theories like EOMCC,[26−29] STEOMCC,[30−32] etc. FCI benchmarks and experimental results are also supplied where available. Section 6 outlines our conclusions and our outlook for the future.

2. THEORETICAL DEVELOPMENTS: THE PARENT UGA-SUMRCC AND ITS QUASI-FOCK (QF) ANALOGUE

We present here a brief summary of the parent UGA-SUMRCC[23] where the aspects of spin-adaptation and termination of the equations become evident. Thereafter, a spin-free valence-specific formulation for direct energy differences which we call UGA-QFMRCC is presented.

2.1. Summary of the UGA-SUMRCC. The objective for formulating the parent UGA-SUMRCC theory[23] was to develop a spin-free theory capable of handling open shell ionized and excited states of a closed shell ground state without spin contamination, while maintaining natural truncation of the direct term and the ease of implementation. This is achieved by taking the following Ansatz for Ω:

$$\Omega = \sum_{\mu} \Omega_{\mu} |\phi_{\mu}\rangle\langle\phi_{\mu}| \tag{1}$$

with

$$\Omega_{\mu} = \{\exp(T_{\mu})\} \tag{2}$$

where the curly bracket above indicates normal ordering with respect to a suitable closed shell vacuum $|0\rangle$. The state $|0\rangle$ is taken in UGA-SUMRCC theory to be the closed shell "core" determinant containing doubly occupied inactive orbitals. The occupancy in $|0\rangle$ is common to all ϕ_{μ}'s. The T_{μ}'s are defined as spin-free unitary generators expressed in terms of spatial orbitals. The ϕ_{μ}'s are unitary group adapted states, which are Gel'fand Configuration State Functions (CSF)[33] of a specific type. They are generated from the vacuum state $|0\rangle$ by unitary group adapted Gel'fand creators. Another qualifier required for ϕ_{μ} is a string of indices collectively denoted as n_{μ} which denotes the occupancies of the orbitals defining ϕ_{μ}. The excited states in our formulation are generated by the action of spin-free unitary generators ($\{\varepsilon_{\mu}^{l}\}$), acting on ϕ_{μ}:

$$|\chi_{\mu}^{l}\rangle = \{\varepsilon_{\mu}^{l}\}|\phi_{\mu}\rangle \tag{3}$$

where $\{\varepsilon_{\mu}^{l}\}$ are in normal order with respect to $|0\rangle$. The functions χ_{μ}^{l} are CSFs but they are neither Gel'fand states nor the SU2 adapted CSFs of Li and Paldus.[17] $\{\varepsilon_{\mu}^{l}\}$'s are linearly independent specific combinations of spatial orbital replacement operators, $\{E_{\mu}^{l}\}$, which are generators of the unitary group. The final working equations involve matrix elements between ϕ_{μ}'s wherein reduced density matrices (RDM) appear which incorporate the spin information of the target state, and hence how we choose the excited CSFs does not play an important role.

As we have mentioned in section 1, our focus is on electron attached/detached and excited states of closed shell ground states, which can be considered as one-particle (1p)/one-hole (1h) and one-hole−one-particle (1h−1p) sectors with respect to the closed shell state considered as a vacuum, respectively. 1h and 1p model spaces are by construction complete. The 1h−1p model spaces are said to be "quasi-complete,"[35] which is a special case of incomplete model spaces (IMS). It was shown by Mukherjee quite some years ago[36−38] that, to maintain size extensivity for IMS, it is necessary to abandon Intermediate Normalization (IN) of Ω. Interestingly, it was also demonstrated in the context of VUMRCC[34] that for the special case of 1h−1p model spaces, both considering and not considering intermediate normalization leads to the same Bloch equation for those cluster operators which contribute to H_{eff}. As it turns out, for the UGA-SUMRCC, such is not the case,[40] although the necessary modification in the Bloch equation abandoning IN is fairly straightforward. Thus, the same set of modules as needed to construct the working equations for cluster amplitudes as well as H_{eff} can more or less be used for the generalization of the formalism for CMS. Thus, operationally speaking, we may organize the solution of our working equation in a way quite analogous to that for a CMS.

To generate the working equations for 1h−1p IMS, we start out from the Bloch equation:

$$H\Omega P = \Omega PPH_{\text{eff}}P = \Omega PH_{\text{eff}}P \tag{4}$$

where H_{eff} is defined recursively from the model space projection of eq 4

$$PH\Omega P = P\Omega PH_{\text{eff}}P \tag{5}$$

For the quasi-complete 1h−1p IMS, all the excitation operators T_{μ} appearing in $\Omega_{\mu} = \{\exp(T_{\mu})\}$ have the interesting property that T_{μ} can never lead to a transition to any model function ϕ_{λ} by its action on ϕ_{μ}: $\langle\phi_{\lambda}|T_{\mu}|\phi_{\mu}\rangle = 0$. This property is exploited to effect the minor modifications necessary in the UGA-SUMRCC for the h−p IMS, even if IN for Ω_{μ} is not valid. Substituting the Ansatz for Ω_{μ} in eq 4, we obtain

$$\{\exp(T_{\mu})\overline{H}_{\mu}\}|\phi_{\mu}\rangle = \sum_{\nu}\{\exp(T_{\nu})\exp(\overline{T_{\nu})W_{\nu\mu}}\}|\phi_{\mu}\rangle \tag{6}$$

$$\{\exp(T_{\mu})\overline{H}_{\mu}\}|\phi_{\mu}\rangle = \sum_{\nu}\{\exp(T_{\mu})\exp(-T_{\mu})\exp(T_{\nu})\exp(\overline{T_{\nu})W_{\nu\mu}}\}|\phi_{\mu}\rangle \tag{7}$$

where

$$\overline{H}_\mu = \overbrace{H \exp(T_\mu)} \tag{8}$$

is a compact notation of the series:

$$\overline{H}_\mu = \{H\} + \{\overbrace{HT_\mu}\} + \frac{1}{2}\{\overbrace{\overbrace{HT_\mu}T_\mu}\} + \ldots \tag{9}$$

The "contraction," $\overbrace{AB}$, connecting two strings of operators A and B denotes the sum of all possible contractions involving all pairs of operators from both A and B. Terms like $\{\overbrace{\overbrace{HT_\mu}T_\mu}\}$ etc. involve contractions between H and the various T_μ's, excluding contractions between the operators of different T_μ's.

The operator, $W_{\nu\mu}$, is a closed operator labeled by orbitals distinguishing ϕ_μ and ϕ_ν. It transforms ϕ_μ to ϕ_ν via the relation

$$W_{\nu\mu}|\phi_\mu\rangle = |\phi_\nu\rangle\langle\phi_\nu|H_{\text{eff}}|\phi_\mu\rangle \tag{10}$$

It is composed of operators of various ranks, the lowest rank being the number of orbitals by which μ and ν differ. $W_{\nu\mu}$ may also contain components with any number of spectator scatterings involving creation and destruction of common active orbitals of ϕ_μ and ϕ_ν, resulting in the ranks of the operator being higher. The spectators need not all be diagonal, it is only essential for the labels of the spectators to be one of the common orbitals of μ and ν.

Equation 7 is satisfied if we invoke the following equality:[23]

$$\{\overline{H}_\mu\}|\phi_\mu\rangle - \sum_\nu \{\exp(-T_\mu)\exp(T_\nu)\overbrace{\exp(T_\nu)W_{\nu\mu}}\}|\phi_\mu\rangle = 0 \tag{11}$$

Now, we will define two components from this equation:

$$G_{\mu,ex} = \{\overline{H}_\mu\}_{ex} - \sum_\nu \{\exp(-T_\mu)\exp(T_\nu)\overbrace{\exp(T_\nu)W_{\nu\mu}}\}_{ex} \tag{12}$$

$$G_{\mu,cl} = \{\overline{H}_\mu\}_{cl} - \sum_\nu \{\exp(-T_\mu)\exp(T_\nu)\overbrace{\exp(T_\nu)W_{\nu\mu}}\}_{cl} \tag{13}$$

Here, "ex" refers to the excited and "cl" to the closed component of the operator: an operator, $A_{\mu,\text{ex}}$, excites to virtual functions by its action on ϕ_μ; an operator, $A_{\mu,\text{cl}}$, converts ϕ_μ to a sum of model space functions:

$$A_{\mu,cl}|\phi_\mu\rangle = \sum_\lambda |\phi_\lambda\rangle\langle\phi_\lambda|A_{\mu,cl}|\phi_\mu\rangle \tag{14}$$

Projection of $\langle\phi_\lambda|$ on $G_{\mu,cl}|\phi_\mu\rangle$ gives

$$\langle\phi_\lambda|\{\overline{H}_\mu\}_{cl}|\phi_\mu\rangle - \langle\phi_\lambda|\sum_\nu \{\exp(-T_\mu)\exp(T_\nu)\overbrace{\exp(T_\nu)W_{\nu\mu}}\}_{cl}|\phi_\mu\rangle \equiv R_{cl,\lambda,\mu} = 0 \tag{15}$$

Projecting with $\langle\chi^l_\mu|$ on $G_{\mu,ex}|\phi_\mu\rangle$ leads to

$$\langle\chi^l_\mu|\{\overline{H}_\mu\}_{ex}|\phi_\mu\rangle - \langle\chi^l_\mu|\sum_\nu \{\exp(-T_\mu)\exp(T_\nu)\overbrace{\exp(T_\nu)W_{\nu\mu}}\}_{ex}|\phi_\mu\rangle \equiv R_{ex,l\mu} = 0 \tag{16}$$

Equation 16 is to be used for determining the cluster amplitudes of T_μ. We note that the first term, called the "*direct term*," will necessarily truncate at quartic power in all situations. The second, so-called, "*coupling term*" will also naturally terminate, but the maximum power will be controlled by the rank of the valence sector under consideration.

We may mention here that the lack of IN for Ω requires an iterative solution for H_{eff} via eq 5. In our actual implementation, we have combined this iteration with that used for obtaining the cluster amplitudes of T_μ. We will elaborate on this in section 5.1.

2.2. Formulation of the Quasi-Fock UGA-SUMRCC. The inspiration for the UGA-QFMRCC theory comes from the development of the parent UGA-SUMRCC[23] and the earlier Quasi-Fock theory of Mukhopadhyay and Mukherjee.[39] In the parent UGA-SUMRCC theory, the t-amplitudes required were only those for the target valence sector (say, excited state). Here, our aim is not to obtain the state energy itself but the energy difference with respect to a subduced valence sector (say, ground state). The benefit of a correlated theory for obtaining energy differences lies in the exact analytic cancelation of the common correlation energy of the two states, leading to a treatment of the common correlation terms of both states on equal footing even under truncated schemes. The theory for computing energy differences with respect to the ground state requires an appropriate parametrization of the wave operator where cluster operators inducing correlation of the ground state should also appear explicitly. We use the notation (m,n) to denote an mh−np valence sector and $T^{(m,n)}$ to denote the cluster operators thereof. The theory we will use in this respect first computes the amplitudes for the (0,0) valence sector which generates the cluster operators of the ground state and then—quite unlike the approach of the Fock Space theory—directly computes the amplitudes for the target (m,n) (say, (1,1)) sector. In the FS-MRCC theory, in contrast we would have had to build the target Ω hierarchically, starting from the (0,0) sector of the Fock space, which is spanned by the HF function, taken as the vacuum. The operators $T^{(1,0)}$ and $T^{(0,1)}$ respectively are constructed in the next stage of solution and provide information on the (1,0) and (0,1) sectors of the Fock space. Next comes the operators $T^{(1,1)}$ of the target sector, viz. the h−p model space. Our theory bypasses the (1,0) and the (0,1) sectors, and this is the reason why such a theory has been called a Quasi Fock MRCC (QF-MRCC) in the literature.[39] Our intention is to develop a spin-free UGA version of a QF-MRCC, using the same strategy as has been formulated in our UGA-SUMRCC,[23] for the direct computation of such energy differences as ionization potential (IP), electron affinity (EA), and excitation energy (EE). The performance of such a formulation also provides us some insights regarding the physics incorporated in our excited state calculations using UGA-SUMRCC as against that in the description of the ground state using SRCC.

We should mention here that there exist several closely related theories, viz. Valence Universal MRCC (VUMRCC),[10−13] the so-called double-curly VUMRCC[41] which uses a special combinatoric cluster Ansatz, and Similarity Transformed Equation of Motion Coupled Cluster (STEOMCC).[30−32] VUMRCC and the double curly VUMRCC utilize a valence universal Ω, while all the other methods involve the calculation of ground state amplitudes which are used to transform the Hamiltonian before the computation of the energy differences. UGA-QFMRCC falls in the second category. However, the Ansatz for UGA-QFMRCC is richer in structure, and we expect a better performance. We have also employed different approximate schemes analogous to those in the UGA-SUMRCC for UGA-QFMRCC to see their performance for this method.

In the present formulation, our first assumption is that the ground state is well described by a single reference theory, namely single-reference coupled cluster theory. Therefore, $\exp(T)$ parametrization of the wave operator, acting on the HF function for the ground state is sufficient. We will treat excited states as multireference in a state universal framework, and for the analogous treatment of the common correlation part, the cluster amplitudes will include the exact ground state T's for every model function and the differential correlation will be

treated by the S_μ amplitudes. This idea naturally suggests that our choice of Ansatz for UGA-QFMRCC should be of the form

$$\Omega_\mu = \exp(T)\{\exp(S_\mu)\} \tag{17}$$

We distinguish carefully between the operators T_μ used in UGA-SUMRCC and S_μ introduced here in the context of UGA-QFMRCC. The T_μ's in UGA-SUMRCC represent the actual correlation of the target state contributed by the virtual excitations from ϕ_μ as in the parent UGA-SUMRCC theory. The S_μ's, on the other hand, represent the *differential correlation* and *relaxation* of the state, i.e., the difference in the correlation contribution of T_μ of the target state and the subduced state with respect to which the energy difference is required.

We explain below the theory for excitation energy, but the same considerations apply also to any other energy difference of interest. The ground state T-amplitudes are first calculated for the closed shell reference state and so, the first part of our Ansatz is known. The working equations to be derived are, thus, for S_μ's of the excited state only. As we have emphasized above, the hierarchical generation of the S_μ's going through the various lower valence sectors as in Valence Universal Multireference Coupled Cluster (VUMRCC)[10−13] is entirely bypassed.

Having solved for T, a dressed Hamiltonian is defined as

$$\tilde{H} = \exp(-T)\, H\, \exp(T) \tag{18}$$

$\tilde{H}$ and H_{eff} are now partitioned to separate out the ground state energy.

$$\tilde{H} = E_{\text{gr}} + \bar{H} \tag{19}$$

$$H_{\text{eff}} = E_{\text{gr}} + \bar{H}_{\text{eff}} \tag{20}$$

$$\bar{H}_{\text{eff}\nu\mu} = \langle\phi_\nu|\bar{W}_{\nu\mu}|\phi_\mu\rangle \tag{21}$$

$\bar{W}_{\nu\mu}$ may be considered as the closed operator whose matrix element with respect to $\langle\phi_\nu|$ and $|\phi_\mu\rangle$ corresponds to $\bar{H}_{\text{eff}\nu\mu}$.

Invoking the Bloch equation for the model function ϕ_μ,

$$H\Omega_\mu|\phi_\mu\rangle = \sum_\nu \Omega_\nu|\phi_\nu\rangle\bar{H}_{\text{eff}\nu\mu} \tag{22}$$

$$H\,\exp(T)\,\{\exp(S_\mu)\}|\phi_\mu\rangle = \sum_\nu \exp(T)\,\{\exp(S_\nu)\}|\phi_\nu\rangle\bar{H}_{\text{eff}\nu\mu} \tag{23}$$

and operating with $\exp(-T)$ from the left, we have

$$\exp(-T)\, H\, \exp(T)\, \{\exp(S_\mu)\}|\phi_\mu\rangle = \sum_\nu \{\exp(S_\nu)\}|\phi_\nu\rangle\bar{H}_{\text{eff}\nu\mu} \tag{24}$$

$$\tilde{H}\{\exp(S_\mu)\}|\phi_\mu\rangle = \sum_\nu \{\exp(S_\nu)\}|\phi_\nu\rangle\bar{H}_{\text{eff}\nu\mu} \tag{25}$$

$$\{\exp(S_\mu)\overline{\bar{H}\exp(S_\mu)}\}|\phi_\mu\rangle = \sum_\nu \{\exp(S_\nu)\}|\phi_\nu\rangle H_{eff\nu\mu} \tag{26}$$

Using the definitions in eqs 19−21, we can cancel E_{gr} from either side of eq 26 to give

$$\{\exp(S_\mu)\overline{\bar{H}\exp(S_\mu)}\}|\phi_\mu\rangle = \sum_\nu \{\exp(S_\nu)\overline{\exp(S_\nu)\bar{W}_{\nu\mu}}\}|\phi_\mu\rangle \tag{27}$$

$$\{\exp(S_\mu)\overline{\bar{H}\exp(S_\mu)}\}|\phi_\mu\rangle = \sum_\nu \{\exp(S_\mu)\exp(-S_\mu)\exp(S_\nu)\overline{\exp(S_\nu)\bar{W}_{\nu\mu}}\}|\phi_\mu\rangle \tag{28}$$

$\bar{W}_{\nu\mu}$, just as the operator $W_{\nu\mu}$ as defined in eq 21, is a closed operator which is necessarily labeled by orbitals distinguishing ϕ_μ and ϕ_ν. It consists of operators of various ranks, the lowest rank being the number of orbitals by which μ and ν differ. Let us call them *closed transfer operators without spectators*. However, $\bar{W}_{\nu\mu}$ may contain components with an arbitrary number of spectator scatterings involving creation and destruction of common active orbitals of ϕ_μ and ϕ_ν. In such cases, the ranks of the operator may be higher than that for $\bar{W}_{\nu\mu}$ without spectators, although it scatters from μ to ν. The spectators need not all be diagonal, it is only essential for the labels of the spectators in $W_{\nu\mu}$ to belong to the set of common orbitals of ϕ_μ and ϕ_ν.

Equation 28 is satisfied if the following equality is invoked:

$$\{\overline{\bar{H}\exp(S_\mu)}\}|\phi_\mu\rangle = \sum_\nu \{\exp(S_\nu)\exp(-S_\mu)\overline{\exp(S_\nu)\bar{W}_{\nu\mu}}\}|\phi_\nu\rangle \tag{29}$$

$$\langle\chi_l\{\bar{\bar{H}}\}|\phi_\mu\rangle - \sum_\nu \langle\chi_l|\{\exp(S_\nu)\exp(-S_\mu)\overline{\exp(S_\nu)\bar{W}_{\nu\mu}}\}|\phi_\nu\rangle = 0 \tag{30}$$

After having solved for the amplitudes of $\{S_\mu\}$, we obtain the sought after energy differences, ΔE_k, and the associated coefficients, $\{c_{\mu k}\}$, from the eigenvalue equation:

$$\sum_\nu \bar{H}_{\text{eff}\mu\nu}c_{\nu k} \equiv \sum_\nu \langle\phi_\mu|\bar{W}_{\mu\nu}|\phi_\nu\rangle c_{\nu k} = \Delta E_k c_{\mu k} \tag{31}$$

3. CHOICE OF CLUSTER OPERATORS IN THE CCSD TRUNCATION SCHEMES FOR UGA-SUMRCC AND UGA-QFMRCC

3.1. Use of Nonredundant Excitation Manifold. We begin with the comment that, in the SUMRCC method using the JM Ansatz in a spin−orbital basis, the set of excited functions, $\{\chi_\mu^l\}$, reached by the action of T_μ's on the various model functions ϕ_μ are complete in the sense that for each of the N active model functions, ϕ_μ, if M_μ is the number of virtual functions reached from ϕ_μ, then the total number of cluster amplitudes is $M = \Sigma_\mu M_\mu$. The corresponding dimension of the Hilbert space spanned by the virtual functions for all the N roots is equal to $M_{\text{virt}} = \Sigma_{l_\mu k} N_{l_\mu k}$. Since $N_{l_\mu} = M_\mu$ and the sum over k is exactly equal to the sum over μ, $M_{\text{virt}} = M$ and we have no redundancy in the SUMRCC theory. Moreover, in a spin−orbital formulation, the virtual determinant, χ_μ^l, reached from a model determinant, ϕ_μ, is uniquely specified by the indices of the occupied and unoccupied spin−orbitals in ϕ_μ. In a spin-free UGA-MRCC, one would naturally want to retain the spirit of the spin−orbital based SUMRCC in that one would choose only those operators in ϕ_μ which for a given change of orbital occupancy would lead to just the linearly independent set of χ_μ^l's with the same inactive and active occupancy. Since operators defined in terms of spatial orbitals do not have a one to one correspondence with pairs (χ_μ^l, ϕ_μ), a proper choice of linearly independent operators becomes important. However, an overcompleteness can arise within the excitation manifold for one model function, ϕ_μ when more than one excitation operator leads to the same excited function. An excited function is characterized by the occupancies of the orbitals and the spin coupling among the singly occupied orbitals. Given the number of open shells (singly occupied orbitals) and the net spin of the state, the number of linearly independent (LIN) functions is known, and only as many equations are logically available as there are LIN functions. It thus is logical to choose suitable linearly independent combinations of the various excitation operators of S_μ inducing the same orbital occupancy changes in the set $\{\chi_\mu^l\}$. If this proper selection is not done to attain the exact number of LIN operators and instead every unitary generator is used in T_μ/S_μ to generate excited CSFs, they would

lead to an overcomplete set of virtual functions. Several UGA-based approaches in the context of SUMRCC have been proposed and implemented, mainly by Li and Paldus.[17,33] Paldus and Li had earlier formulated a theory in which Gel'fand–Tsetlin (GT) excited states were generated.[42,43] As the formalisms were rather complex, they had exploited SU2 group adaptation of the generators to form their excitation operators. The generators of Gel'fand states are combined to form the linearly independent operators of an SU2 group. They will not necessarily follow the one-to-one orthogonality relation of the corresponding Gel'fand adapted excited states of an $U(n_c + n_a + n_v)$ group where n_c denotes the number of inactive core orbitals, n_a denotes the number of active (equivalently, valence) orbitals, and n_v denotes the number of inactive virtual orbitals. They argued that, to retain size extensivity, the states must obey this orthogonality relationship. They had also normalized the resulting operators.

In the present formalism, we have generated the working equations by projecting the set of Bloch equations to the excited state CSF's, χ_μ^j. Our operator combinations are LIN although not necessarily orthogonal. The projections naturally lead to the appearance of n-body RDMs in the working equations. The connectedness of the projected equations is sufficient to prove the size-extensivity of our formalism.

We propose to choose our combinations of operators in a practicable manner within the framework of our theory, using a two-pronged approach: a perturbative analysis of our working equations and the knowledge of the number of LIN functions. Whether these operators produce mutually orthogonal virtual functions, $\chi_\mu^{j_i}\ \forall\ i$ is something we do not consider at all. We illustrate our scheme using an example.

We will henceforth denote by labels i, j, ..., etc. the inactive holes; by a, b, ..., etc. the inactive particles; by I, J, ..., etc. the active holes; and by A, B, ..., etc. the active particles. Excitations involving an orbital, "i," and an orbital, "a," can belong to two classes: (i) not involving a change in occupancy of the active hole (I) or particle (A) orbitals or (ii) involving a change in occupancy of the active hole or particle orbitals. t_i^a, t_{il}^{Ia}, and t_{iA}^{Aa} belong to the first class. It is enough if we explain our strategy using the T's belonging to this class. For those belonging to the second class, like t_{ij}^{Aa} or t_{IA}^{ab} etc., an exactly analogous analysis can be used.

To discern which of the excitation operators accompanying the amplitudes, t_i^a, t_{il}^{Ia}, and t_{iA}^{Aa}, are linearly independent, we first construct the projection equations for all of them and look at their algebraic structures. The explicit working equations for t_i^a, t_{il}^{Ia}, and t_{iA}^{Aa} operators in the 1h–1p sector are as follows:

$$\begin{aligned} &G_i^a - G_{iI}^{aI}\eta_I^I + G_{iA}^{aA}\gamma_A^A - \frac{1}{2}G_{iI}^{Ia}\eta_I^I - \frac{1}{2}G_{iA}^{Aa}\gamma_A^A + G_{iIA}^{aIA}\Gamma_{IA}^{IA} \\ &\quad - \frac{1}{2}G_{iAI}^{AaI}\Gamma_{IA}^{IA} - \frac{1}{2}G_{iIA}^{IaA}\Gamma_{IA}^{IA} + G_{iIA}^{aAI}\Gamma_{IA}^{AI} - \frac{1}{2}G_{iIA}^{AaI}\Gamma_{IA}^{IA} \\ &\quad - \frac{1}{2}G_{iAI}^{IaA}\Gamma_{IA}^{AI} = 0 \end{aligned} \tag{32}$$

$$\begin{aligned} &G_i^a\eta_I^I - G_{iI}^{aI}\eta_I^I - G_{iA}^{aA}\Gamma_{IA}^{IA} + 2G_{iI}^{Ia}\eta_I^I - G_{iA}^{Aa}\Gamma_{AI}^{IA} + G_{iIA}^{aIA}\Gamma_{IA}^{IA} \\ &\quad + G_{iIA}^{AIa}\Gamma_{IA}^{AI} - 2G_{iIA}^{IaA}\Gamma_{IA}^{IA} + G_{iIA}^{aAI}\Gamma_{IA}^{AI} - 2G_{IiA}^{aAI}\Gamma_{IA}^{AI} \\ &\quad + G_{iAI}^{IaA}\Gamma_{IA}^{IA} = 0 \end{aligned} \tag{33}$$

$$\begin{aligned} &-G_i^a\gamma_A^A - G_{iI}^{aI}\Gamma_{IA}^{IA} - G_{iA}^{aA}\gamma_A^A - G_{iI}^{Ia}\Gamma_{AI}^{IA} + 2G_{iA}^{Aa}\gamma_A^A - G_{iIA}^{aIA}\Gamma_{IA}^{IA} \\ &\quad + 2G_{iIA}^{AIa}\Gamma_{IA}^{IA} - G_{iIA}^{IaA}\Gamma_{IA}^{AI} - G_{iIA}^{aAI}\Gamma_{IA}^{AI} + 2G_{IiA}^{aAI}\Gamma_{IA}^{AI} \\ &\quad + G_{iAI}^{IaA}\Gamma_{IA}^{IA} = 0 \end{aligned} \tag{34}$$

where

$$\gamma_A^A = \langle\phi_\mu|\{E_A^A\}|\phi_\mu\rangle = 1$$
$$\eta_I^I = 2 - \langle\phi_\mu|\{E_I^I\}|\phi_\mu\rangle = 2 - \gamma_I^I = 1 \tag{35}$$
$$\Gamma_{IA}^{IA} = \langle\phi_\mu|\{E_{IA}^{IA}\}|\phi_\mu\rangle = -1$$
$$\Gamma_{IA}^{AI} = \langle\phi_\mu|\{E_{IA}^{AI}\}|\phi_\mu\rangle = 1 + (-1)^S \tag{36}$$

where S is the spin of the CSF, ϕ_μ (i.e., $S = 0$ for singlet and $S = 1$ for triplet). To obtain the LIN combinations of operators, it is sufficient to consider up to two-body G-blocks. For the singlet excited states, using the values of the RDMs as in eq 35, we arrive at the following equations:

$$G_i^a - G_{iI}^{aI} + G_{iA}^{aA} + \frac{1}{2}G_{iI}^{Ia} - \frac{1}{2}G_{iA}^{Aa} = 0 \tag{37}$$

$$G_i^a - G_{iI}^{aI} + G_{iA}^{aA} + 2G_{iI}^{Ia} - 2G_{iA}^{Aa} = 0 \tag{38}$$

$$G_i^a - G_{iI}^{aI} + G_{iA}^{aA} + 2G_{iI}^{Ia} - 2G_{iA}^{Aa} = 0 \tag{39}$$

Similarly, the equations for triplet states are

$$G_i^a - G_{iI}^{aI} + G_{iA}^{aA} + \frac{1}{2}G_{iI}^{Ia} - \frac{1}{2}G_{iA}^{Aa} = 0 \tag{40}$$

$$G_i^a - G_{iI}^{aI} + G_{iA}^{aA} + 2G_{iI}^{Ia} = 0 \tag{41}$$

$$G_i^a - G_{iI}^{aI} + G_{iA}^{aA} - 2G_{iA}^{Aa} = 0 \tag{42}$$

We note here that eq 38 and eq 39 are identical. Thus, t_{iI}^{Ia} and t_{iA}^{Aa} are linearly dependent operators. After a slight mathematical manipulation, the set of equations can be equivalently written as

$$G_i^a - G_{iI}^{aI} + G_{iA}^{aA} = 0 \tag{43}$$

$$G_{iI}^{Ia} - G_{iA}^{Aa} = 0 \tag{44}$$

The first order perturbative estimate of the cluster amplitude t_i^a from eq 43 is given by

$${}^1T_i^{a(1)} \approx \frac{(f_i^a - V_{iI}^{aI} + V_{iA}^{aA})\{E\}}{f_i^i - V_{iI}^{iI} + V_{iA}^{iA} - f_a^a + V_{aI}^{aI} - V_{aA}^{aA}} = {}^1t_i^{a(1)}\{E\} \tag{45}$$

Similarly, eq 44 indicates that

$${}^2t_i^{a(1)} \approx \frac{(V_{iI}^{Ia} - V_{iA}^{Aa})}{f_i^i - V_{iI}^{iI} + V_{iA}^{iA} - f_a^a + V_{aI}^{aI} - V_{aA}^{aA}} \tag{46}$$

The quantities f_p^p ($p = i$ or a) are orbital energies, and V_{rs}^{pq} are the two-body matrix elements. Thus, the corresponding operators, $\{E_{iI}^{Ia}\}$ and $\{E_{iA}^{Aa}\}$, should be treated on the same footing in a combination as guided by the first order estimate. We should therefore introduce ${}^2T_i^a \equiv {}^2t_i^a[\{E_{iI}^{Ia}\} - \{E_{iA}^{Aa}\}]$ with a common amplitude ${}^2t_i^a$ as the unknown and use eq 44 for its determination.

Thus the first class of operators contains ${}^1t_i^a\{E_i^a\}$ and ${}^2T_i^a \equiv {}^2t_i^a[\{E_{iA}^{Aa}\} - \{E_{iI}^{Ia}\}]$. Similarly, the second class of operators

contains ${}^2\tilde{T}_i^a = {}^1\tilde{t}_i^a[\{E_{iI}^{aA}\} - 0.5\{E_{iI}^{Aa}\}]$ and ${}^2\tilde{T}_i^a = {}^2\tilde{t}_i^a[\{E_{iA}^{aI}\} - 0.5\{E_{iA}^{Ia}\}]$.

The triplet equations, on the other hand, do not indicate any linear dependence, and hence, all three amplitudes, t_i^a, t_{iI}^{Ia}, and t_{iA}^{Aa} can be used.

A comparative list of Paldus and our operators is provided in Tables 1 and 2, wherein the operators chosen by Li and Paldus[17] have been converted to normal order with respect to the HF function for an easy comparison with our manifold of operators.

Table 1. Choices of *T*'s for Singlet 1h−1p States

	UGA-SUMRCC	OSCC (Paldus and Li)[17]
T_i^I	$t_i^I\{E_i^I\}$	$t_i^I\{E_i^I\}$
T_i^A	$t_i^A\{E_i^A\}$	$t_i^A\{E_i^A\}$
T_I^a	$t_I^a\{E_I^a\}$	$t_I^a\{E_I^a\}$
T_A^a	$t_A^a\{E_A^a\}$	$t_A^a\{E_A^a\}$
${}^1T_i^a$	${}^1t_i^a\{E_i^a\}$	$\frac{1}{\sqrt{2}}\,{}^1t_i^a\{E_i^a\}$
${}^2T_i^a$	${}^2t_i^a[\{E_{iA}^{Aa}\} - \{E_{iI}^{Ia}\}]$	$\frac{1}{\sqrt{2}}\,{}^2t_i^a[\{E_{iI}^{Ia}\} - \{E_{iA}^{Aa}\} - \{E_i^a\}]$
$T_{ij}^{\bullet\bullet}$	$t_{ij}^{\bullet\bullet}[\{E_{ij}^{IA}\} + \{E_{ij}^{AI}\}]$	$\frac{1}{\sqrt{2}}t_{ij}^{\bullet\bullet}[\{E_{ij}^{IA}\} + \{E_{ij}^{AI}\}]$
$T_{\bullet\bullet}^{ab}$	$t_{\bullet\bullet}^{ab}[\{E_{IA}^{ab}\} + \{E_{AI}^{ab}\}]$	$\frac{1}{\sqrt{2}}t_{\bullet\bullet}^{ab}[\{E_{IA}^{ab}\} + \{E_{AI}^{ab}\}]$
$\tilde{T}_i^a$	${}^1\tilde{t}_i^a[\{E_{iI}^{aA}\} - 0.5\{E_{iI}^{Aa}\}]$	${}^1\tilde{t}_i^a[\{E_{iI}^{aA}\} + \{E_{iI}^{Aa}\}]$
	${}^2\tilde{t}_i^a[\{E_{iA}^{aI}\} - 0.5\{E_{iA}^{Ia}\}]$	${}^2\tilde{t}_i^a[\{E_{iA}^{aI}\} + \{E_{iA}^{Ia}\}]$
T_{ii}^{aa}	$t_{ii}^{aa}\{E_{ii}^{aa}\}$	$\frac{1}{2}t_{ii}^{aa}\{E_{ii}^{aa}\}$
T_{ii}^{ab}	$t_{ii}^{ab}\{E_{ii}^{ab}\}$	$\frac{1}{\sqrt{2}}t_{ii}^{ab}\{E_{ii}^{ab}\}$
T_{ij}^{aa}	$t_{ij}^{aa}\{E_{ij}^{aa}\}$	$\frac{1}{\sqrt{2}}t_{ij}^{aa}\{E_{ij}^{aa}\}$
T_{ij}^{ab}	$t_{ij}^{ab}\{E_{ij}^{ab}\}$	$\frac{1}{2}\,{}^1t_{ij}^{ab}[\{E_{ij}^{ab}\} + \{E_{ij}^{ba}\}]$
	$t_{ij}^{ba}\{E_{ij}^{ba}\}$	$\frac{1}{2\sqrt{3}}\,{}^2t_{ij}^{ab}[\{E_{ij}^{ab}\} - \{E_{ij}^{ba}\}]$

Table 2. Choices of *T*'s for Triplet 1h−1p States

	UGA-SUMRCC	OSCC (Paldus and Li)[17]
T_i^I	$t_i^I\{E_i^I\}$	$t_i^I\{E_i^I\}$
T_i^A	$t_i^A\{E_i^A\}$	$t_i^A\{E_i^A\}$
T_I^a	$t_I^a\{E_I^a\}$	$t_I^a\{E_I^a\}$
T_A^a	$t_A^a\{E_A^a\}$	$t_A^a\{E_A^a\}$
T_i^a	$t_i^a\{E_i^a\}$	$\frac{1}{\sqrt{2}}\,{}^1t_i^a\{E_i^a\}$
T_{iI}^{Ia}	$t_{iI}^{Ia}\{E_{iI}^{Ia}\}$	$\frac{1}{\sqrt{2}}\,{}^2t_i^a[\{E_{iI}^{Ia}\} - \{E_{iA}^{Aa}\} - \{E_i^a\}]$
T_{iA}^{Aa}	$t_{iA}^{Aa}\{E_{iA}^{Aa}\}$	$\frac{1}{2}\,{}^3t_i^a[\{E_{iI}^{Ia}\} + \{E_{iA}^{Aa}\}]$
$T_{ij}^{\bullet\bullet}$	$t_{ij}^{\bullet\bullet}[\{E_{ij}^{IA}\} - \{E_{ij}^{AI}\}]$	$\frac{1}{2}t_{ij}^{\bullet\bullet}[\{E_{ij}^{IA}\} - \{E_{ij}^{AI}\}]$
$T_{\bullet\bullet}^{ab}$	$t_{\bullet\bullet}^{ab}[\{E_{IA}^{ab}\} - \{E_{AI}^{ab}\}]$	$\frac{1}{2}t_{\bullet\bullet}^{ab}[\{E_{IA}^{ab}\} - \{E_{AI}^{ab}\}]$
T_{iI}^{Aa}	$t_{iI}^{Aa}\{E_{iI}^{Aa}\}$	$t_{iI}^{Aa}\{E_{iI}^{Aa}\}$
T_{ij}^{aI}	$t_{ij}^{aI}\{E_{ij}^{aI}\}$	$\frac{1}{\sqrt{2(1+\delta_{ij})}}\,{}^1t_{ij}^{aI}[\{E_{ij}^{aI}\} + \{E_{ji}^{aI}\}]$
T_{ji}^{aI}	$t_{ji}^{aI}\{E_{ji}^{aI}\}$	$\frac{1}{\sqrt{6}}\,{}^2t_{ij}^{aI}[\{E_{ji}^{aI}\} - \{E_{ij}^{aI}\}]$
T_{ij}^{aA}	$t_{ij}^{aA}\{E_{ij}^{aA}\}$	$\frac{1}{\sqrt{2(1+\delta_{ij})}}\,{}^1t_{ij}^{aA}[\{E_{ij}^{aA}\} + \{E_{ji}^{aA}\}]$
T_{ji}^{aA}	$t_{ji}^{aA}\{E_{ji}^{aA}\}$	$\frac{1}{\sqrt{6}}\,{}^2t_{ij}^{aA}[\{E_{ji}^{aA}\} - \{E_{ij}^{aA}\}]$
T_{iI}^{ab}	$t_{iI}^{ab}\{E_{iI}^{ab}\}$	$\frac{1}{\sqrt{2(1+\delta_{ab})}}\,{}^1t_{iI}^{ab}[\{E_{iI}^{ab}\} + \{E_{iI}^{ba}\}]$
T_{iI}^{ba}	$t_{iI}^{ba}\{E_{iI}^{ba}\}$	$\frac{1}{\sqrt{6}}\,{}^2t_{iI}^{ba}[\{E_{iI}^{ba}\} - \{E_{iI}^{ba}\}]$
T_{iA}^{ab}	$t_{iA}^{ab}\{E_{iA}^{ab}\}$	$\frac{1}{\sqrt{2(1+\delta_{ab})}}\,{}^1t_{iA}^{ab}[\{E_{iA}^{ab}\} + \{E_{iA}^{ba}\}]$
T_{iA}^{ba}	$t_{iA}^{ba}\{E_{iA}^{ba}\}$	$\frac{1}{\sqrt{6}}\,{}^2t_{iA}^{ba}[\{E_{iA}^{ba}\} - \{E_{iA}^{ba}\}]$
T_{ii}^{aa}	$t_{ii}^{aa}\{E_{ii}^{aa}\}$	$\frac{1}{2}t_{ii}^{aa}\{E_{ii}^{aa}\}$
T_{ii}^{ab}	$t_{ii}^{ab}\{E_{ii}^{ab}\}$	$\frac{1}{\sqrt{2}}t_{ii}^{ab}\{E_{ii}^{ab}\}$
T_{ij}^{aa}	$t_{ij}^{aa}\{E_{ij}^{aa}\}$	$\frac{1}{\sqrt{2}}t_{ij}^{aa}\{E_{ij}^{aa}\}$
T_{ij}^{ab}	$t_{ij}^{ab}\{E_{ij}^{ab}\}$	$\frac{1}{2}\,{}^1t_{ij}^{ab}[\{E_{ij}^{ab}\} + \{E_{ij}^{ba}\}]$
T_{ij}^{ba}	$t_{ij}^{ba}\{E_{ij}^{ba}\}$	$\frac{1}{2\sqrt{3}}\,{}^2t_{ij}^{ab}[\{E_{ij}^{ab}\} - \{E_{ij}^{ba}\}]$

3.2. Deliberate Use of Sufficiency Conditions. In the previous subsection, we have seen that suitable combinations of operators need to be chosen to ensure a linearly independent excitation manifold. This would become increasingly complicated as we proceed to higher valence sectors. There is a possibility that inflating the number of equations by invoking sufficiency conditions would allow us to use all possible unitary generators (E) without having to bother about what combination to use. We explore this possibility for a 1h−1p sector using both UGA-SUMRCC and UGA-QFMRCC. The true benefit of this scheme is, however, expected to be in the extension of these theories to higher valence sectors and higher body T operators. In the context of the example mentioned in section 2.1, this would mean using the following set of equations:

$$G_i^a - G_{iI}^{aI} + G_{iA}^{aA} - G_{iIA}^{aIA} + 2G_{iIA}^{aAI} - G_{iAI}^{IaA} = 0 \tag{47}$$

$$G_{iI}^{Ia} + G_{iIA}^{IaA} - G_{IiA}^{aAI} = 0 \tag{48}$$

$$G_{iA}^{Aa} - G_{iIA}^{AIa} + G_{IiA}^{aAI} = 0 \tag{49}$$

Similarly, the equations for the other dependent operators may be separated out. The excitation manifold here is overcomplete with the same function generated more than once. Unlike the space of Gel'fand adapted excited functions, our manifold in the parent UGA-SUMRCC is linearly independent but nonorthogonal. On invoking sufficiency, the operators become linearly independent. A possible hurdle is the independent evaluation of dependent amplitudes which might destroy the relative contribution of these amplitudes. The performance of this approximation with artificial inflation of unknowns and equations has thus to be carefully assessed to test its efficacy. The results are presented in section 5.3.

3.3. Treatment of Orbital Relaxation and Differential Correlation for Excitation Energies (EE) in UGA-QF vs Allied Theories. Whenever multiple valence sectors are involved in the description of a state, it is pertinent to discuss the physics incorporated in a theory for direct determination of excitation energy (EE) under three headings: (1) an appropriate choice of the wave operator for the excited state which ensures exact cancellation

of the correlated ground state energy in the EE, (2) orbital relaxation of the ground state orbitals, and (3) differential correlation. The two latter points describe the changes attendant on excitation. Since the formulation of our UGA-QFMRCC shares all the three characteristics 1−3 above with the Fock-space MRCC (FS-MRCC),[10−13] Eigenvalue Independent Partitioning (EIP) in Fock space (FS-EIP),[56] and the Similarity Transformed Equation of Motion CC (STEOM-CC) theory,[30−32] it is pertinent to have a comparative perspective of all these theories.

All four theories use the factorized cluster Ansatz for the wave operator of the excited state:

$$\Omega = \exp(T)\Omega_v \tag{50}$$

where $\exp(T)$ is the wave operator for the ground state in the CC form and Ω_v introduces the effects of valence correlation, core−valence interaction, and orbital relaxation/differential correlation. It is in the quantitative inclusion of the various physical effects induced by Ω_v that the four theories differ. The factorized cluster Ansatz allows the complete cancellation of the ground state correlation energy via the use of the dressed Hamiltonian, $\tilde{H}$ of eq 18, which allows a clean separation of the ground state energy E_{gr} and the operator part of $\tilde{H}$, $\bar{H}$, as shown in eq 19. Thus, for the same truncation scheme for the ground state, the magnitude of the ground state energy subtracted for all four theories is exactly the same. The effective Hamiltonian, $\bar{H}_{\text{eff}}$ generating the energy differences depends on Ω_v which may be different for the four theories. This is reflected in eq 21 where $\bar{H}_{\text{eff}}$ depends on Ω_v, which may be different for the four theories in actual applications. The FS-MRCC, FS-EIP, and STEOM-CC all invoke the concept of valence universality[10] and express Ω_v as

$$\Omega_v = \{\exp S\} \tag{51}$$

where S consists of cluster operators of different valence sectors: $S = S^{(0,1)} + S^{(1,0)} + S^{(1,1)}$. $S^{(m,n)}$ are the valence cluster operators involving destruction of "m" holes and "n" electrons occupying the mh and np active orbitals. In the FS-MRCC, the $S^{(1,0)}$ and $S^{(0,1)}$ amplitudes are solved to get the information on the IP and EA sectors, respectively. The additional correlation, including the dispersion interaction between the active hole and particle for the (1,1) sector, is taken care of by the $S^{(1,1)}$ cluster amplitudes. In the FS-EIP, the Bloch equation for every valence sector is cast into an eigenvalue equation obtained in the union space of $\{\phi_\mu^{(m,n)}\}$, and the set $\{\chi_\mu^{I(m,n)} \equiv \varepsilon^{I(m,n)}\phi_\mu^{(m,n)}\}$ where $\{\phi_\mu^{(m,n)}\}$ denotes the set of model functions for the (m,n) sector and the set $\{\chi_\mu^{I(m,n)}\}$ are the virtual functions obtained by the action of excitation operators $\varepsilon^{I(m,n)}$ on $\phi_\mu^{(m,n)}$. In STEOM-CC, a technique similar to FS-EIP is used with the proviso of an approximation that the $S^{(1,1)}$ amplitudes are ignored altogether. In our UGA-QFMRCC, all the cluster operators are for the (1,1) sector, and there is no hierarchical build-up through the (0,1) and (1,0) sectors to the (1,1) sector. An advantage of FS-EIP or STEOM-CC, as currently implemented, lies in that the (1h, 0p) and (0h,1p) valence sector equations can be exactly cast as a matrix eigen-problem, enabling easy and intruder-free evaluation of S amplitudes. Although in principle, our UGA-QFMRCC also can be cast as a matrix eigen-problem, thereby obviating intruders in a similar manner, we have not implemented such a strategy yet. We tend to look upon the transcription of the set of Bloch equations to the matrix eigen-problem as a technique to handle intruders.

The strength of the UGA-QFMRCC theory lies in the model-function dependence of the S amplitudes (the so-called μ dependence), which eliminates altogether the artificial use of higher rank S amplitudes with direct spectator scatterings. This in itself ensures that all the S amplitudes have knowledge of all the valence occupancies of the model functions. If we refer to the Ansatz of our wave operator in eq 17, the factorized Ansatz $T\exp\{S_\mu\}$ for the component Ω_μ of the wave operator acting on ϕ_μ ensures that not only the ground state dressing via exp T of the Hamiltonian makes the direct computation of excitation energy possible but also it allows us to use S amplitudes involving excitations only while incorporating the involvement of all the active holes and particles present in ϕ_μ. As an example, an operator S_μ inducing excitation from $i \rightarrow a$ for a function ϕ_μ with active occupancy (I,A) subsumes in it interaction with I and A separately as spectators as also the interactions where I and A are both involved.

As depicted in Figure 1, single excitations like E_i^a, E_{iA}^{aA}, and E_{iA}^{Aa} among others are involved in correction of orbitals for

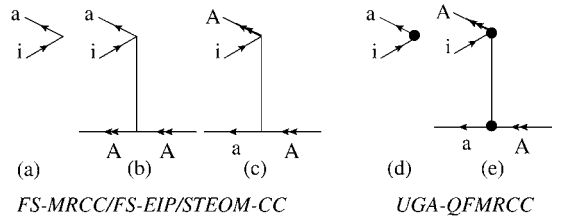

Figure 1. FS-MRCC/FS-EIP/STEOM-CC (a,b) vs UGA-QFMRCC (d,e)-Orbital relaxation diagrams. Note that for the (0,1) sector and the target (1,1) sector, the operator in b from normal-ordered Ω_v terminates at linear power while d subsumes a and b and, thus, occurs to all powers. Following the usual convention, inactive lines are denoted by single arrows, and the active lines are denoted by double arrows. The filled circle vertex in parts d and e depict the model space dependence of the inactive excitation operator of S_μ.

model spaces where A is an active virtual orbital (say, for a 1p or 1h−1p model space). In FS-MRCC or FS-EIP/STEOM-CC, E_{iA}^{aA}, E_{iA}^{Aa}, E_{iI}^{aI}, and E_{iI}^{Ia}, which are responsible for orbital relaxation due to change in valence occupancy, are present up to linear power only while in UGA-QFMRCC; the set of operators E_i^a, E_{iA}^{aA}, E_{iI}^{aI}, E_{iIA}^{aIA}, and E_{iIA}^{aAI} are clubbed together as $\varepsilon_i^{a(\mu)}$ (denoted with bold vertices in Figure 2, which occurs to all powers.

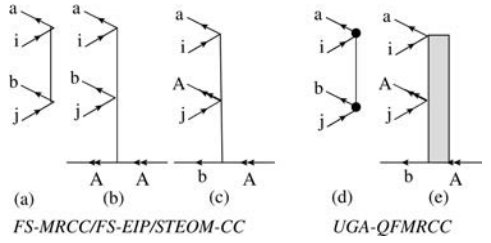

Figure 2. FS-MRCC/FS-EIP/STEOM-CC vs UGA-QFMRCC-Differential correlation. Note that for the (0,1) sector, the operators b and c from normal-ordered Ω_v are necessary for introducing differential correlation but are absent in a singles−doubles truncation while d subsumes a and b and, thus, occurs to all powers. The operator, c is absent in UGA-QFMRCC, but some implicit contribution through the G-block shown in e is possible.

Hence, physics is incorporated to a greater extent in UGA-QFMRCC on two counts: (a) knowledge of the S amplitudes regarding the valence occupancies I and A and (b) a full exponential involving $S_{\mu i}^a$ (with $\phi_\mu \equiv \phi_I^A$). When E_{iA}^{Aa} is LIN with E_i^a, however, it occurs up to linear power even in UGA-QFMRCC. The correlation on the other hand is incorporated by the two-body excitation operators and differential correlation by three-body operators with direct and exchange spectators as in Figure 2. Thus, in FS-MRCC or FS-EIP/STEOM-CC, a CCSD

truncation scheme has no such differential correlation operators while the UGA-QFMRCC easily incorporates the direct spectator contributions to all orders. The exchange spectator blocks implicitly contribute in the projection equations. Other than spectator scatterings, orbital relaxation and correlation relaxation also occur in the presence of multiple valence occupancies. In order to fully include all such contributions, it would be necessary to use up to $(m + n + 2)$ rank operators for an (m,n)-valence sector such as in Figure 3, which is not a practical possibility in

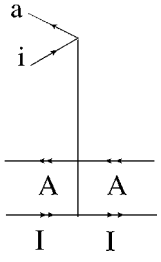

Figure 3. FS-MRCC/FS-EIP/STEOM-CC vs UGA-QFMRCC-Orbital relaxation for the (1,1) sector. This would, in principle, require such a three-body operator from a normal-ordered Ω_v, which is implicitly present in the $T^a_{\mu i}$ of our UGA-QFMRCC.

FS-MRCC/FS-EIP/STEOM-CC with spectator scattering of "m" holes and "n" particles in both direct and exchange modes. However, the direct spectator scatterings in the FS-MRCC can be subsumed in UGA-QFMRCC with low body excitation operators labeled by the CSF index, μ, and such operators can be treated to all powers. The operators with some exchange spectator scatterings would still be having higher ranks than just the excitation ranks, but—unlike in FS-MRCC/FS-EIP/STEOM-CC—μ dependence via inclusion of higher body blocks would not necessitate the inclusion of all the spectator labels. Some other excitations like E^I_i and E^a_A will terminate at the linear power in both theories. If we ignore three and higher body excitations (exchange spectators, in particular), in FS theories they then never appear in the Bloch equation. In contrast, although the three/four body S_μ's also do not appear in UGA-QFMRCC, the corresponding blocks do, enriching the physical content implicitly in UGA-QFMRCC. In STEOM-CC, as mentioned above, one ignores the $S^{(1,1)}$ amplitudes, and it would miss the dispersion interaction in the wave function. Since our working equations have G-blocks with I and A both interacting, the dispersion interaction is incorporated. Inclusion of such multiple spectators becomes particularly relevant for the description of differential correlation accompanying excitation. We can simply introduce μ-dependent double excitations of the type $ij \rightarrow ab$, while in EIP/STEOM-CC we would need at least a three-body operator with spectator active scattering or even a four-body operator with the pairs of I and A. Absence of this differential correlation in a truncated CCSD scheme is evident in the computed energies from EIP or STEOM-CC vis-a-vis UGA-QFMRCC. This is a general advantage of any theory based on or derived from the Jeziorski−Monkhorst Ansatz as against the Valence-Universal Ansatz. Moreover the Quasi-Fock formalism has cluster amplitudes for just the (0,0) and (1,1) sectors, thereby bypassing entirely the necessity of having to go through the 1h−0p and 0h−1p sectors before reaching the target, 1h−1p sector. The number of cluster amplitudes in UGA-QFMRCC is thus less than that in EIP or STEOM-CC to include equivalent physics, which is further enhanced by the possibility of the appearance of all powers of S_μ which do not have exchange spectators. This would be best demonstrated in situations where orbital relaxation is very high, such as core electron ionization and excitation. Preliminary investigations indicate that UGA-QFMRCC is considerably better than EOM-CC in these cases, although COS-CC[20] is even better, as expected.

4. SIZE EXTENSIVITY OF THE PARENT UGA-SUMRCC AND EVALUATION OF SIZE INTENSIVE ENERGIES IN UGA-QFMRCC

In this section, we recapitulate the aspects of size extensivity of UGA-SUMRCC and further elaborate on how the connectedness of equations with apparently disconnected terms arising from the occurrence of n-body RDMs solely on one fragment of a projected composite may be demonstrated to be actually connected. There are two levels of connectivity to be analyzed. First, we must demonstrate that the G blocks themselves are connected composites. Next, we must be able to show that the different components of the working equations obtained on projection by $\langle\chi^l_\mu|$ are connected among themselves. Since RDMs are not in general connected quantities, we must conclusively show that all of the terms in the matrix element $\langle\chi^l_\mu|G^{l(n)}_\mu|\phi_\mu\rangle$, with the potential of being disconnected, either necessarily have common labels with the G blocks or cancel on algebraic manipulation. In essence, one needs to show that the terms contributing to each projection equation are connected entities and the cluster amplitudes of the set T_μ are connected.

4.1. Connectivity of the G_μ Blocks. To start with, we assume that the cluster amplitudes are connected and analyze the connectivity of the G blocks. The G blocks in eqs 12 and 13 are composed of two types of terms, the so-called "*direct term*" and the "*coupling term*." The composite quantity, $\bar{H}_\mu$, is an explicitly connected quantity if T_μ's are connected. Hence, the direct terms are connected. For the coupling term, we have to analyze several different aspects of the connectivity:

(1) Connectivity of $\overline{\exp(T_\nu)W_{\nu\mu}}$: $W_{\nu\mu}$ consists of those closed components of $\bar{H}_\mu$ which excites ϕ_μ to ϕ_ν and being a part of $\bar{H}_\mu$ is explicitly connected. For connected T_ν's, $\overline{\exp(T_\nu)W_{\nu\mu}}$ is explicitly connected. In what follows, we will henceforth denote $\overline{\exp(T_\nu)W_{\nu\mu}}$ as $X_{\nu\mu}$

(2) Connectivity of $\{\exp -(T_\mu - T_\nu)X_{\nu\mu}\}$: We consider two possible cases here: the case where ϕ_ν and ϕ_μ differ by at least one orbital (case 2a) and the case where ϕ_μ and ϕ_ν have the same orbital occupancy and either $\phi_\mu = \phi_\nu$ or they differ in the spin coupling scheme of the active orbitals (case 2b).

For case 2a, the quantity $X_{\nu\mu}$ is explicitly dependent on all the active orbitals by which ϕ_μ and ϕ_ν differ since $X_{\nu\mu}$ contains $W_{\nu\mu}$. Since all the CSFs in the model spaces are treated on the same footing, the functional dependence of every cluster amplitude on the active orbital labels remains the same. Hence, the difference of the amplitudes $t_\mu - t_\nu$ inducing the same excitation depends implicitly on one or more of the active orbitals by which ϕ_μ and ϕ_ν differ. Hence, the composite $\{\exp-(T_\mu - T_\nu)X_{\nu\mu}\}$ has at least one common active orbital label shared by the two factors, and hence, the composite is connected. We also note here that our analysis subsumes the case where the action of some components of T_ν on ϕ_μ is zero in the coupling term in eq 12 because of the occupancy restrictions of some active orbitals. Clearly, the corresponding T_μ involving the same label of active orbitals in creation and destruction must involve those orbitals by which ϕ_μ and ϕ_ν differ.

For case 2b, if ϕ_μ and ϕ_ν are the same, the composite in the coupling term reduces simply to $X_{\nu\mu}$, which is obviously connected. If ϕ_μ and ϕ_ν have the same orbital occupancy but differ in their spin coupling schemes, then the quantity $X_{\nu\mu}$ would depend

on one or more of the same orbitals involved in the different spin couplings for ϕ_μ and ϕ_ν. In such a situation, the difference $t_\mu - t_\nu$ will have implicit dependence on all active orbitals involved in the segments in which the spin couplings of ϕ_μ and ϕ_ν are different.

4.2. Connectivity of the Working Equations Involving $\{\varepsilon_l^\mu\}$ and G_μ. The second level of connectivity, that of the working equation, requires more sophisticated analyses. We first note that the various ranks n of $G_\mu^{l(n)}$ can contribute to a matrix element, $\langle\chi_\mu^l|G_\mu^l|\phi_\mu\rangle\langle\chi_\mu^l|\Sigma_n G_\mu^{l(n)}|\phi_\mu\rangle$. Using eq 3, we may express the matrix element as expectation values with respect to ϕ_μ:

$$\langle\chi_\mu^l|\sum_n G_\mu^{l(n)}|\phi_\mu\rangle = \langle\phi_\mu|\{\varepsilon_\mu^l\}^\dagger\sum_n G_\mu^{l(n)}|\phi_\mu\rangle \equiv \langle\phi_\mu|\{\varepsilon_l^\mu\}\sum_n G_\mu^{l(n)}|\phi_\mu\rangle \tag{52}$$

Using Wick's theorem to rewrite the product of $\{\varepsilon_l^\mu\}$ with those appearing in $G_\mu^{l(n)}$, it is easy to see that the only non-zero contribution to the matrix element comes from the terms which are either completely contracted or those involving unitary generators with active labels only. The latter will give rise to RDMs of various ranks dependent on the rank of the unitary generators with active labels. We note now that the set of active orbital labels destroyed by the unitary generators must be the same as those created although they are not necessarily in the same order. For example, with $\phi_\mu \equiv \phi(I,A)$, the non-zero 2-RDMs can only be Γ_{IA}^{IA} and Γ_{IA}^{AI}. We would henceforth refer to strict index equality in the lower and upper indices as "*diagonality*." When the upper and lower index sets are equal but not all of the equal labels are in the same order in the upper and lower sets, we refer to this property as "*quasi-diagonality*." Hence, Γ_{IA}^{IA} is diagonal and Γ_{IA}^{AI} is quasi-diagonal. In our UGA-SUMRCC, all density matrix elements are either diagonal or quasi-diagonal.

For the h−p model spaces studied by us here, the non-zero 2-RDMs are not always product separable, and they may lead to disconnected pieces in various terms. The disconnected pieces appear when a part of the pairs of active orbitals appears only on the de-excitation part of the operator, $\{\varepsilon_l^\mu\}$, and a part on the G block or when all the pairs of active orbitals of the RDM come from the $\{\varepsilon_l^\mu\}$ only. Representative diagrams for the first case are shown in Figures 4 and 5. In a CCSD truncation

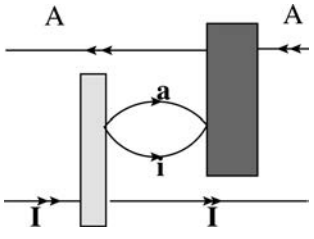

Figure 4. Apparently disconnected term when I and A are on different fragments. We note here that the left-most projection operator is a de-excitation operator and is *not* associated with a connected amplitude. Hence, one would have to keep in mind that it is not a connected entity, unlike the G blocks on the right. The same holds good for the de-excitation operators in Figures 5 and 6.

scheme for an h−p quasi-complete model space, some active lines to the right may emanate from the G block and have common labels with active lines to the left which may have arisen from the projection which are the problematic situation depicted in Figures 4 and 5. Even though parts of the 2-RDM may occur on different factors ($\{\varepsilon_l^\mu\}$ and $G_\mu^{l(n)}$; as in Figure 5), they are by necessity quasi-diagonal and hence connected. As a consequence,

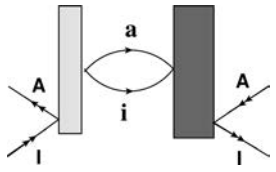

Figure 5. Apparently disconnected term with quasi-diagonal RDM.

when the factors $\{\varepsilon_l^\mu\}$ and $G_\mu^{l(n)}$ each have an h−p pair on them, the labels on the h−p lines are the same leading to connected structures. A term like Figure 4 does not occur in our formulation, as we do not have T operators containing direct spectators, and hence, there are no projection equations with $\{\varepsilon_l^\mu\}$ having its adjoint structure. However, we do have the so-called exchange spectator operators, and terms like Figure 6 arise which can

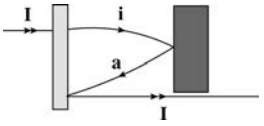

Figure 6. Occurrence of disconnected RDM and excitation.

apparently cause disconnected terms when the label, I, and the pair, i,a, are on different molecular fragments.

Our intention is to demonstrate that one can eliminate the disconnected terms via cumulant decomposition. We shall show that the disconnected quantities for a given working equation get canceled on invoking the working equations for other, lower rank, t-amplitudes. In order to match terms between equations, it becomes necessary to decompose higher body densities into lower body densities via a so-called cumulant decomposition.[44] We will also demonstrate that in order to factor out the lower body equation from the higher body equation in its entirety, we need to introduce terms containing higher body densities which are zero in value. The strategy used by us is general and may be suitably extended for analyzing the extensivity for general mh−np quasi-complete model spaces.

We define the 1h density matrix element η_I^I as

$$\eta_I^I = \sum_\sigma = \langle\phi_\mu|I_\sigma I_\sigma^\dagger|\phi_\mu\rangle = -\langle\phi_\mu|\{E_I^I\}|\phi_\mu\rangle = 1$$

γ_A^A is obviously equal to $\langle\phi_\mu|\{E_A^A\}|\phi_\mu\rangle = 1$. Using the general definition of a spin-free cumulant,[44] we have

$$\Gamma_{wx}^{uv} = \langle\phi_\mu|\{E_w^u\}|\phi_\mu\rangle\langle\phi_\mu|\{E_x^v\}|\phi_\mu\rangle - \frac{1}{2}\langle\phi_\mu|\{E_x^u\}|\phi_\mu\rangle\langle\phi_\mu|\{E_w^v\}|\phi_\mu\rangle + \Lambda_{wx}^{uv} \tag{53}$$

$$\begin{aligned}\Gamma_{xyz}^{uvw} = {} & \langle\phi_\mu|\{E_u^x\}|\phi_\mu\rangle\langle\phi_\mu|\{E_v^y\}|\phi_\mu\rangle\langle\phi_\mu|\{E_w^z\}|\phi_\mu\rangle \\ & - \frac{1}{2}\langle\phi_\mu|\{E_u^x\}|\phi_\mu\rangle\langle\phi_\mu|\{E_w^y\}|\phi_\mu\rangle\langle\phi_\mu|\{E_v^z\}|\phi_\mu\rangle \\ & + \langle\phi_\mu|\{E_u^x\}|\phi_\mu\rangle\Lambda_{vw}^{yz} - \frac{1}{2}\langle\phi_\mu|\{E_w^x\}|\phi_\mu\rangle\langle\phi_\mu|\{E_v^y\}|\phi_\mu\rangle \\ & \times\langle\phi_\mu|\{E_u^z\}|\phi_\mu\rangle + \langle\phi_\mu|\{E_v^y\}|\phi_\mu\rangle\Lambda_{uw}^{xz} \\ & - \frac{1}{2}\langle\phi_\mu|\{E_v^x\}|\phi_\mu\rangle\langle\phi_\mu|\{E_u^y\}|\phi_\mu\rangle\langle\phi_\mu|\{E_w^z\}|\phi_\mu\rangle \\ & + \langle\phi_\mu|\{E_w^z\}|\phi_\mu\rangle\Lambda_{uv}^{xy} + \frac{1}{4}\langle\phi_\mu|\{E_w^x\}|\phi_\mu\rangle\langle\phi_\mu|\{E_u^y\}|\phi_\mu\rangle \\ & \times\langle\phi_\mu|\{E_v^z\}|\phi_\mu\rangle + \frac{1}{4}\langle\phi_\mu|\{E_v^x\}|\phi_\mu\rangle\langle\phi_\mu|\{E_w^y\}|\phi_\mu\rangle \\ & \times\langle\phi_\mu|\{E_u^z\}|\phi_\mu\rangle + \Lambda_{uvw}^{xyz}\end{aligned} \tag{54}$$

for arbitrary active indices $u-z$, which may be holes or particles. We then find that

$$\Gamma^{IA}_{IA} = -\eta^{I}_{I}\gamma^{A}_{A} + \Lambda^{IA}_{IA} \tag{55}$$

$$\Gamma^{AI}_{IA} = \frac{1}{2}\eta^{I}_{I}\gamma^{A}_{A} + \Lambda^{AI}_{IA} \tag{56}$$

For the h−p CSFs, it then follows that Λ^{IA}_{IA} is zero and Λ^{AI}_{IA} is non-zero, indicating that Γ^{AI}_{IA} is not exactly factorizable into products of lower body RDMs.

To ascertain the connectivity of the working equations, by the strategy delineated in the paragraphs where the η^{I}_{I}'s are defined, let us consider the specific example of the pair of projection equations for t^{a}_{i} and t^{Ia}_{iI}, i.e., eqs 32 and 33. We note that the active label, I, in the de-excitation operator, E^{Ii}_{aI}, will always contribute an RDM where I will figure in both the upper and lower indices. Among the various terms generated in the projection equations, there will be some terms containing η^{I}_{I} while the rest of the terms will contain either Γ^{IA}_{IA} or Γ^{AI}_{IA}. The latter two can also be written in terms of factors η^{I}_{I} and γ^{A}_{A} and a cumulant, Λ, if we use eqs 55 and 56. Thus, the entire set of projection equations can be grouped into two parts: in one, η^{I}_{I} explicitly appears, and in the other, only Λ^{IA}_{IA} or Λ^{AI}_{IA} but no η^{I}_{I} appears. It is then possible to rewrite eq 33 as

$$\begin{aligned}
&\eta^{I}_{I}\Big[\boldsymbol{G^{a}_{i}} - G^{aI}_{iI} + 2G^{Ia}_{iI} + \gamma^{A}_{A}(-\boldsymbol{G^{aA}_{iA}} + G^{aIA}_{iIA} - 2G^{IaA}_{iIA} + G^{IaA}_{iAI}) \\
&- \frac{1}{2}\gamma^{A}_{A}(-\boldsymbol{G^{Aa}_{iA}} + G^{AaI}_{iAI} + G^{aAI}_{iIA} - 2G^{AaI}_{iIA})\Big] \\
&(\text{term } i) \\
&+\Lambda^{IA}_{IA}(-G^{aA}_{iA} + G^{aIA}_{iIA} - 2G^{IaA}_{iIA} + G^{IaA}_{iAI}) \\
&+ \Lambda^{AI}_{IA}(-G^{Aa}_{iA} + G^{AaI}_{iAI} + G^{aAI}_{iIA} - 2G^{AaI}_{iIA}) = 0 \\
&(\text{term } ii)
\end{aligned} \tag{57}$$

We note that in term i there are several components in which the pair of lines containing label I are generated exclusively from the de-excitation operator, E^{Ii}_{aI}. *These components are all disconnected, and they are all characterized by the property that the label I, never appears in the associated G blocks.* These disconnected entities have been shown in bold letters. It is remarkable that all the components in term i appearing in the brackets, (...) in eq 57 appear in eq 32 which originates from the projection with E^{i}_{a}. However, there are more components in eq 32 than what appears in term i. The missing entities in term i are those in eq 32 which contain: (a) η^{I}_{I} and (b) the 2-RDMs, Γ^{IA}_{IA} and Γ^{AI}_{IA}. These terms obviously cannot appear in term i, since this would have required a cumulant decomposition of a 2-RDM, Γ^{II}_{II} for a, and 3-RDMs in eq 33 containing at least one "I" in both its upper and lower indices. For h−p CSFs, Γ^{II}_{II} and all the 3-RDMs are zero since such density matrices would have violated the exclusion principle in a ϕ_{μ} where there are only single active hole and particle occupancies labeled by I and A, respectively. In order to complete the appearance of all components of eq 32 in term i, we add to eq 33 all those components which contain Γ^{II}_{II} and 3-RDMs which do not change the equation since they are all zero in value. We thus add the following sum of components, each of which is individually zero:

$$\begin{aligned}
&-G^{Ia}_{iI}\Gamma^{II}_{II},\ -G^{AaI}_{iAI}\Gamma^{AII}_{IAI},\ -G^{aIA}_{iIA}\Gamma^{IAI}_{IAI},\ -G^{aAI}_{iIA}\Gamma^{IAI}_{IIA},\ -G^{AaI}_{iAI}\Gamma^{IAI}_{IAI}, \\
&-G^{IaA}_{iIA}\Gamma^{AII}_{IAI},\ -G^{IaA}_{iAI}\Gamma^{AII}_{IAI}
\end{aligned} \tag{58}$$

Equation 33 thus becomes

$$\begin{aligned}
&G^{a}_{i}\eta^{I}_{I} - G^{aI}_{iI}\eta^{I}_{I} - G^{aI}_{iI}\Gamma^{II}_{II} - G^{aA}_{iA}\Gamma^{IA}_{IA} + 2G^{Ia}_{iI}\eta^{I}_{I} - G^{Ia}_{iI}\Gamma^{II}_{II} \\
&- G^{Aa}_{iA}\Gamma^{IA}_{AI} + G^{aIA}_{iIA}\Gamma^{IA}_{IA} + G^{AIa}_{iIA}\Gamma^{AI}_{IA} - 2G^{IaA}_{iIA}\Gamma^{IA}_{IA} \\
&+ G^{aAI}_{IiA}\Gamma^{AI}_{IA} - 2G^{aAI}_{IiA}\Gamma^{AI}_{IA} + G^{IaA}_{iAI}\Gamma^{IA}_{IA} - G^{AaI}_{iAI}\Gamma^{AII}_{IAI} \\
&- G^{aIA}_{iIA}\Gamma^{IAI}_{IAI} - G^{aAI}_{iIA}\Gamma^{IAI}_{IIA} - G^{AaI}_{iAI}\Gamma^{IAI}_{IAI} - G^{IaA}_{iIA}\Gamma^{AII}_{IAI} \\
&- G^{IaA}_{iAI}\Gamma^{AII}_{IAI} = 0
\end{aligned} \tag{59}$$

The cumulant decomposition of the zero RDMs would generate either a product of cumulants containing an η^{I}_{I} and some 2-Λ or a product of 1-RDMs, one of which would be η^{I}_{I}, or a 3-Λ. In fact, the cumulant decomposition of the associated zero 2- and 3-RDMs have the expressions:

$$\Gamma^{II}_{II} = 0 = \frac{1}{2}{\eta^{I}_{I}}^{2} + \Lambda^{II}_{II} \tag{60}$$

$$\Gamma^{AII}_{IAI} = 0 = -\frac{1}{4}{\eta^{I}_{I}}^{2}\gamma^{A}_{A} - \eta^{I}_{I}\Lambda^{AI}_{IA} + \Lambda^{IAI}_{AII} \tag{61}$$

$$\Gamma^{IAI}_{IAI} = 0 = \frac{1}{2}{\eta^{I}_{I}}^{2}\gamma^{A}_{A} - 2\eta^{I}_{I}\Lambda^{IA}_{IA} + \gamma^{A}_{A}\Lambda^{II}_{II} + \Lambda^{IAI}_{IAI} \tag{62}$$

Using the expressions above, we can include the missing components of eq 32 in term i (to be henceforth called modified term i) and club the rest of the contribution of eq 58 into term ii (to be henceforth called modified term ii). We show explicitly only the terms containing two body G blocks to avoid complexity. The decomposition of the higher body densities using eqs 35−62 can be similarly carried out.

$$\begin{aligned}
&\eta^{I}_{I}\Big[G^{a}_{i} - G^{aI}_{iI}\eta^{I}_{I} + G^{aA}_{iA}\gamma^{A}_{A} - \frac{1}{2}G^{Ia}_{iI}\eta^{I}_{I} - \frac{1}{2}G^{Aa}_{iA}\gamma^{A}_{A}\Big] \\
&(\text{modified term } i) \\
&+ \left(\frac{1}{2}{\eta^{I}_{I}}^{2} - \eta^{I}_{I} - \Lambda^{II}_{II}\right)G^{aI}_{iI} + \left(-\frac{1}{2}{\eta^{I}_{I}}^{2} + 2\eta^{I}_{I} - \Lambda^{II}_{II}\right)G^{Ia}_{iI} \\
&- \Lambda^{IA}_{IA}G^{aA}_{iA} - \Lambda^{AI}_{IA}G^{Aa}_{iA} = 0 \\
&(\text{modified term } ii)
\end{aligned} \tag{63}$$

Owing to the validity of eq 32, the entire modified term i vanishes, making eq 33 reduce to just the modified term ii for up to two body G blocks:

$$\begin{aligned}
&\left(\frac{1}{2}{\eta^{I}_{I}}^{2} - \eta^{I}_{I} - \Lambda^{II}_{II}\right)G^{aI}_{iI} + \left(-\frac{1}{2}{\eta^{I}_{I}}^{2} + 2\eta^{I}_{I} - \Lambda^{II}_{II}\right)G^{Ia}_{iI} - \Lambda^{IA}_{IA}G^{aA}_{iA} \\
&- \Lambda^{AI}_{IA}G^{Aa}_{iA} = 0
\end{aligned} \tag{64}$$

Since, 2- and 3-Λ's are all size extensive quantities, eq 33 written in terms of the cumulants, Λ, consists entirely of connected terms. Some components in the modified term ii contain only 3-Λ's, and their size extensivity ensures that each such component is connected. There would also be some contribution coming from products of γ^{A}_{A} and a 2-Λ where the γ^{A}_{A} always occurs on the G block. Hence, these components are also connected. By an entirely similar reasoning, eq 39 involving the de-excitation operator E^{Ai}_{aA} upon cumulant decomposition would also reduce to a set of connected components involving cumulants after invoking eq 32. Here, the roles of γ^{A}_{A} and η^{I}_{I} would be interchanged. Moreover, also for true excitations involving active orbitals (such as $I \rightarrow a$ or $i \rightarrow a$), the projection equations involving an exchange spectator scattering in the de-excitation operator can be also similarly transformed into a

set of connected components containing appropriate 2-Λ's and 3-Λ's. The disconnected components along with several other connected components and appropriate densities vanish because of the validity of the lower body equations without the spectators. Turning now to the one-body projection equations, the uncontracted active lines in a composite may appear either entirely on the G block which is explicitly connected or one on the projection and the other on the G block. In the latter case, diagonality/quasi-diagonality of RDMs ensures that they are connected since the active line on the de-excitation operator would have one label in common with one of those occurring on the G block.

It is interesting to note that the proof of the connectivity brought to the fore the use of 2- and 3-Λ's having indices for which the corresponding 2- and 3-Γ's vanish due to the Pauli exclusion principle. This is clearly demonstrated in eqs 60−62 above. We may call such cumulants Exclusion Principle Violating (EPV) Λ's. For the h−p case at the CCSD level of truncation, the connected expressions will contain up to 3-Λ's. For higher truncation schemes, 4- and higher rank Λ's can also appear.

The same conclusions could have been drawn by an alternative but equivalent strategy. If we include in a projection equation, such as eq 33, all the possible higher body RDMs, $n > 2$ in our case, and use cumulant decompositions for all of them, then, in general, all the disconnected terms cancel out because of the validity of lower body equations, leaving us with connected terms and higher body cumulants. Clearly, this method will prove to be more profitable for the general mh−np case. We note that although in our h−p model spaces, all higher body Λ's are of the EPV type, such is not the case of a general mh−np active space. The alternative strategy introduced above becomes then much easier for the purpose of discerning connectivity.

Since the above two strategies are equivalent for proving the connectedness of the working equations, in our actual implementation we have used the parent projection equations like eq 33. Solving eqs 32 and 33 is equivalent to solving eqs 32 and 64, and the same is true for other projection equations. We must, however, bear in mind that, although the n-body RDM elements corresponding to the EPV types are zero, the corresponding n-body Λ's are necessarily not so. Hence, in order to adopt this scheme, one must start with all possible RDMs, *even those of ranks beyond the number of active electrons*, in the parent projection equations. For the h−p case, the vanishing Γ_3's are actually implicitly included (though only formally so).

The structure of the UGA-QFMRCC equations are exactly analogous to the UGA-SUMRCC equations where $\bar{H}$ replaces H and $\bar{W}$ replaces W. Both $\bar{H}$ and $\bar{W}$ are connected quantities, and therefore like UGA-SUMRCC, UGA-QFMRCC also gives connected equations. Following the prescription of Mukherjee et al.,[34] we can say that, as UGA-QFMRCC gives connected working equations, ΔE calculated from this theory is size intensive.

5. MOLECULAR APPLICATIONS

5.1. Computational Organizations. Three different but closely related theories have been discussed in this paper. The final working equation for obtaining the cluster amplitudes in the parent UGA-SUMRCC is eq 16.

To incorporate the lack of IN of Ω_μ in the definition of H_{eff}, we will use the expression for H_{eff} as in section 5.1 and put it back into eq 10 at each step of iteration. Using eq 15, at any iterative step $(i + 1)$, we can write:

$$\langle \phi_\lambda | \{\overline{H}_\mu^{(i)}\}_{cl} | \phi_\mu \rangle - \langle \phi_\lambda | \sum_\nu \{(\exp(-T_\mu)\exp(T_\nu) - 1)(\exp(\overbrace{T_\nu}) - 1) W_{\nu\mu}^{(i)}\}_{cl} \tag{65}$$

$$+ \{(\exp(-T_\mu)\exp(T_\nu) - 1) W_{\nu\mu}^{(i)}\}_{cl} | \phi_\mu \rangle = H_{eff,\lambda\mu}^{(i+1)} \tag{66}$$

where

$$W_{\nu\mu}^{(i)} | \phi_\mu \rangle = | \phi_\nu \rangle \langle \phi_\nu | H_{\text{eff}}^{(i)} | \phi_\mu \rangle \tag{67}$$

We start the iteration of H_{eff} with the following expression:

$$H_{\text{eff},\lambda\mu}^{(0)} = \bar{H}_{\lambda\mu}^{(0)} = H_{\lambda\mu} \tag{68}$$

Here, an important point to notice is that, in each step of iteration, we have chosen our H_{eff} in such a manner that it corresponds to the true solution for the residue eq 15:

$$R_{cl,\lambda\mu} = 0 \tag{69}$$

Subsequently, we will diagonalize H_{eff} to get the energies for all the "k" states.

To implement the sufficiency variant of the parent UGA-SUMRCC, we have separated out the blocks corresponding to linearly dependent operators. Then, the residues for each operator are computed, and iteration is performed until the residue becomes zero. The algorithm for H_{eff} for the sufficiency variant is exactly the same as that for the parent UGA-SUMRCC.

For UGA-QFMRCC, we need to generate all possible $\overbrace{He^{S_\mu}}$ connected terms which is called $\bar{H}$. Then, we should construct all possible $\overbrace{He^{S_\mu}}$ connected diagrams to get G blocks of which the excitation structures contribute to S_μ's and the closed diagrams contribute to H_{eff}. S_μ's are the differential amplitudes for the target valence sector. In our implementation technique, our goal has been to generate all diagrams possible in $\overbrace{He^{S_\mu}}$ connected without going through the explicit construction of all possible $\bar{H}$'s. The scheme is as follows:

(1) Write all the converged closed shell T's in a file.
(2) Read from the file and map the T's to the indices of the model functions. Thus, now the range of the T array is generalized hole−particle, with entries in valid locations and the rest zero.
(3) Add the T to S_μ and treat it as a composite array called S_μ'.
(4) Evaluate all possible $\overbrace{He^{S_\mu'}}$ connected diagrams.This gives us the correct set of required diagrams.
(5) Construction of $\bar{H}_{\text{eff}}$: We pick up the IP-like, EA-like, and EE-like portions from the G blocks. We also calculate the following closed diagrams where V is connected to the closed shell T's and T-like differential S_μ's:

$$(\overbrace{FS_{1\mu}}), (\overbrace{VS_{2\mu}}), (\overbrace{VS_{1\mu}^2}), (\overbrace{VT_1S_{1\mu}})$$

The sum of these two portions yields $\bar{H}_{\text{eff}}$ at each step of iteration (i). For the implementation of 5, we calculate $(\overbrace{FS_{1\mu}'})$, $(\overbrace{VS_{2\mu}'})$, and $(\overbrace{VS_{1\mu}'^2})$ and subtract from it the closed shell correlation energy at each iteration step. The algorithm for $\bar{H}_{\text{eff}}$ is exactly the same as for the parent UGA-SUMRCC after replacing H_{eff} by $\bar{H}_{\text{eff}}$ and $W_{\nu\mu}$ by $\bar{W}_{\nu\mu}$. Diagonalization of the final $\bar{H}_{\text{eff}}$ yields excitation energies directly.

5.2. Computational Cost. The computational cost of UGA-QFMRCC must be studied stepwise. The first step is simply a CCSD calculation. The next transformation by S_μ involves a cost of roughly N_{dim} times a CCSD computation where N_{dim} is the number of model functions.

At each step, the scaling with the number of basis functions, N, is dominated by the computations involving all-particle integrals, VPPPP. The number of unknowns scale as $N_{gh}{}^4N_{gp}{}^2$ where gh (generalized hole) = the number of occupied orbitals + the number of active orbitals and gp (generalized particle) = the number of unoccupied orbitals + the number of active orbitals. The most expensive part of our computation is the construction of three-body G blocks which involve a cost of $6(\text{nact})^2$ times a CCSD computation where "nact" is the number of active orbitals and there are six possible three body structures for the G blocks given one active hole, I, and one active particle, A. The overall scaling behavior of our UGA-QFMRCC is in fact of the same order as those in EIP or STEOM-CC except that the STEOM-CC ignores the three-body excitation operators necessary for equivalence, of physics incorporated, with our UGA-QFMRCC as mentioned in section 3.3. This is an approximation, and such approximations are open to us as well. Due to the compact μ-dependent representation of the cluster operators, it was not necessary for us to try this simplification. Since, this is a theory for N_{dim} states without much superfluous cost, we believe that the theory is workable in situations where accuracy takes precedence over computational cost for small to medium molecules.

5.3. Results and Discussions. To demonstrate the performance of "sufficiency conditions" and our new quasi-Fock formulation, we present some representative computations. Work is underway to obtain more data for a more conclusive demonstration of the strengths and weaknesses of this theory. We would like to draw the attention of the readers to the fact that some UGA-SUMRCC values presented here differ from those reported in our previous paper.[23] This is due to some small bugs in our earlier code. The conclusions of our previous publication, however, remain unchanged. We have chosen excited states of H_2O, HF, CH_2, BH, and CH^+ for theoretical comparisons in small bases. Appropriate bar charts have been presented to compare the trends in results for the parent UGA-SUMRCC (scheme P) and its variant (scheme S) where sufficiency conditions have been employed. Tables are presented to demonstrate the better performance of UGA-QFMRCC in comparison with EOMCC and the comparable performance of UGA-QFMRCC and the parent UGA-SUMRCC. Subsequently, we present excitation energies in comparison with experimental results for H_2O and C_2H_2. All unreferenced results have been computed by us using GAMESS US- 2007 or -2010.[45] Results of EOM-CCSD for triplet states have been obtained using DALTON 2.0.[46]

Molecular Specifications. In the present section, we describe the molecular geometry, active spaces, and basis sets considered for our computations. The geometries for comparison with experimental results are mentioned as footnotes to the corresponding tables. The H_2O molecule has been studied in DZV and cc-PVnZ (n = D,T,Q) bases at the ground state equilibrium geometry: O(0, 0, 0), H(0, ± 0.751155, −0.581606) in Å. The model space of H_2O contains $(3a_1, 1b_1)$ orbitals from the occupied level and $(4a_1, 2b_2)$ orbitals from the unoccupied level in all of our applications in the present paper.

The excitation energies for the singlet and triplet Π states of HF have been computed using the DZV and cc-PVnZ (n = D,T,Q) bases at a bond length of 1.40 au. For HF, we have considered the two lowest energy degenerate functions of B1 and B2 symmetry in our model space.

The coordinates for CH_2 have been taken as C(0, 0, 0), H(0, ± 0.87251610, −0.67314164) in Å. For this molecule, our choice of model space consists of the $3a_1$ orbital from the occupied set of orbitals and $(4a_1,1b_1)$ from the unoccupied orbitals.

Computations for BH have been carried out at a bond length of 2.3289 au using cc-PVnZ (n = D,T,Q) bases. We have chosen the $(3a_1)$ orbital from the occupied set of orbitals and $(1b_1,1b_2)$ orbitals from the virtual set for the construction of our model space.

CH^+ has been treated at its equilibrium geometry of 2.137280 au. The bases we have used for this computation

Table 3. Scheme S − Scheme P in mH: Difference between Use of Sufficiency Conditions and Use of Linearly Independent Manifold of Operators

molecule	state	cc-pVDZ	cc-pVTZ	cc-pVQZ
HF	$^1\Pi$	−1.776	−1.889	−1.992
	$^3\Pi$	−0.959	−1.24	−1.258
H_2O	$^1B_1$	−2.751	−2.638	−2.656
	$^1A_2$	−1.689	−1.888	−2.206
	$^1A_1$	−2.197	−1.792	−1.639
	$^1B_2$	−2.234	−2.025	−1.977
	$^3B_1$	−0.959	−1.009	−1.049
	$^3A_2$	0.206	−0.077	−0.413
	$^3A_1$	−0.336	−0.343	−0.446
	$^3B_2$	0.111	−0.099	−0.332
CH_2	$^1B_1$	0.887	0.108	0.212
	$^3B_1$	1.668	0.529	0.316
CH^+	$^1\Pi$	0.346	0.858	2.653
	$^3\Pi$	0.933	1.016	1.77

Table 4. Statistical Data for Percent Error of S vs P

	[(abs(S − P))/P]*100	[(S − P)/P]*100
mean	0.00175	0.00078
SD	0.00143	0.00214
max diff	0.00699	0.00362
min diff	0.00010	−0.00699

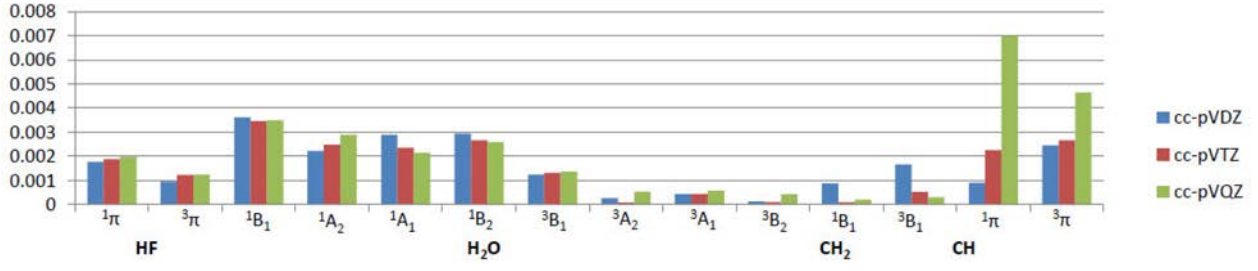

Figure 7. Bar chart showing absolute percent error of scheme S vs scheme P in UGA-SUMRCC.

Table 5. Singlet Excited States of H_2O Using DZV Basis

method	$^1B_1$	M-FCI (mH)	$^1A_2$	M-FCI (mH)	$^1A_1$	M-FCI (mH)	$^1B_2$	M-FCI (mH)
scheme P	−75.816863	1.399	−75.740235	1.819	−75.729277	1.461	−75.640250	3.152
scheme S	−75.817596	0.666	−75.741435	0.619	−75.730500	0.238	−75.643499	−0.097
scheme P′	−75.816449	1.813	−75.741057	0.997	−75.730466	0.272	−75.641504	1.898
scheme S′	−75.816489	1.773	−75.740798	1.256	−75.730253	0.485	−75.640936	2.466
EOM-CCSD	−75.821486	−3.224	−75.744183	−2.129	−75.733449	−2.711	−75.644781	−1.379
FCI	−75.818262		−75.742054		−75.730738		−75.643402	

Table 6. Triplet Excited States of H_2O Using DZV Basis

method	$^3B_1$	M-FCI (mH)	$^3A_2$	M-FCI (mH)	$^3A_1$	M-FCI (mH)	$^3B_2$	M-FCI (mH)
scheme P	−75.845827	0.356	−75.759085	0.491	−75.763853	0.957	−75.688871	1.896
scheme S	−75.845315	0.868	−75.758776	0.800	−75.763417	1.393	−75.689339	1.428
scheme P′	−75.843931	2.252	−75.757459	2.117	−75.763212	1.598	−75.688797	1.970
scheme S′	−75.843689	2.494	−75.757756	1.820	−75.762718	2.092	−75.689800	0.967
EOM-CCSD	−75.849656	−3.473	−75.761222	−1.646	−75.767952	−3.142	−75.692649	−1.882
FCI	−75.846183		−75.759576		−75.764810		−75.690767	

Table 7. Singlet and Triplet Excited States of HF Using DZV Basis

method	$^1\Pi$	M-FCI	$^3\Pi$	M-FCI (mH)
scheme P	−99.580710	2.218	−99.603656	1.328
scheme S	−99.581510	1.418	−99.604007	0.977
scheme P′	−99.580289	2.639	−99.602395	2.589
scheme S′	−99.580383	2.545	−99.602908	2.076
EOM-CCSD	−99.591057	−8.130	−99.613134	−8.150
FCI	−99.582928		−99.604984	

are cc-PVnZ (n = D,T,Q). Here, our choice of model space contains two degenerate function of B_1 and B_2 symmetry.

Use of Nonredundant vs Redundant Excitations. The scheme using sufficiency equations (denoted as scheme S) is tested for excited states of several molecules. On comparing with the full scheme (denoted as scheme P) where only a linearly independent excitation space is used, it appears that consistency is lacking for scheme S across different molecules. However, error ranges are not very high. A further approximation where three-body G blocks with double-exchange spectators whose operator structure corresponds to three body T's as per our policy are neglected is also explored. This scheme is called scheme S′. The performance of this approximation in scheme S is found to follow the trend of performance of scheme P′ which involves a similar approximation in scheme P. We may thus independently analyze the issue of importance of higher body G blocks appearing at higher orders of perturbation and the use of sufficiency conditions in the working equations. As demonstrated in our previous paper,[23] the contribution of four-body blocks is on the order of tenths of a mH and may be neglected for preliminary investigations. The scheme denoted as scheme P2 in our previous paper[23] is denoted as scheme P in this paper as G blocks up to three-body have only been considered for all computations.

To represent the efficacy of the sufficiency variant of UGA-SUMRCC in comparison with the parent theory, we resort to the following sets of data/charts:

(1) Table 3 shows the difference in energy between the two variants along the cc-PVnZ series of basis (where n = D,T,Q) separately for excited states of H_2O, HF, CH_2, BH, and CH^+ molecules. Several states of both singlet and triplet multiplicities have been considered. Clearly, we expect a range of difference values across different bases and states, but this should be small for the viability of scheme S. Since the state energies for different molecules are extensive quantities, we have compared the percent deviation of S vs P in this reasonably large sample space of 42 data points. The bar chart in Figure 7 pictorially represents these data. Statistical data like mean, absolute mean, and standard deviation from absolute mean have been extracted to inspect the systematism (please refer to Table 4).

(2) To investigate how both the variants behave with respect to the FCI energy (where available), we have presented tables where deviation from FCI for each method has been provided (Tables 5−10).

(3) To analyze the change in error with a systematic increase in basis size, we compare the standard deviation of the percent gain in correlation energy from cc-pVDZ to cc-pVTZ and from cc-pVTZ to cc-pVQZ across our sample space separately for the full projection scheme (P) and the variant using sufficiency (S).

The bar chart in Figure 7 for different molecules shows very consistent results. A few outliers are the $^1A_2$ and $^1B_2$ states of H_2O in the cc-pVDZ basis, which are of opposite trend from rest of the bases (please refer to Table 3).

Table 8. Singlet and Triplet Excited States of CH_2 Using cc-pVDZ Basis

method	$^1B_1$	M-FCI (mH)	$^1A_1$	M-FCI (mH)	$^3B_1$	M-FCI (mH)	$^3A_1$	M-FCI (mH)
scheme P	−38.962073	0.275	−38.722847	1.545	−39.033638	−2.611	−38.742057	2.564
scheme S	−38.961186	1.162	−38.723192	1.200	−39.031970	−0.943	−38.742228	2.393
scheme P′	−38.965121	−2.773	−38.725365	−0.970	−39.032726	−1.699	−38.741833	2.788
scheme S′	−38.962776	−0.428	−38.724279	0.113	−39.032367	−1.340	−38.741978	2.643
EOM-CCSD	−38.959034	3.314	−38.720011	4.381	−39.028531	2.496	−38.740466	4.155
FCI	−38.962348		−38.724392		−39.031028		−38.744621	

Table 9. Singlet and Triplet Excited States of BH Using cc-pVDZ Basis

method	$^1\Pi$	M-FCI (mH)	$^3\Pi$	M-FCI (mH)	$^1\Sigma_1$	M-FCI (mH)	$^3\Sigma_1$	M-FCI (mH)
scheme P	−25.105068	0.132	−25.169890	−1.299	−24.851627	−1.126	−24.914764	3.061
scheme S	−25.103118	2.082	−25.167822	0.769	−24.850924	−0.423	−24.908551	9.274
scheme P′	−25.108466	−3.266	−25.170172	−1.581	−24.851432	−0.931	−24.913651	4.174
scheme S′	−25.104499	0.701	−25.169678	−1.087	−24.848211	2.290	−24.910691	7.134
EOM-CCSD	−25.102518	2.682	−25.166993	1.598	−24.847535	2.966	−24.913286	4.539
FCI	−25.105200		−25.168591		−24.850501		−24.917825	

Table 10. Singlet and Triplet Excited States of CH^+ Using cc-pVDZ Basis

method	$^1\Pi$	M-FCI (mH)	$^3\Pi$	M-FCI (mH)
scheme P	−37.886484	−0.358	−37.962947	−1.606
scheme S	−37.886138	−0.012	−37.962014	−0.673
scheme P′	−37.891325	−5.199	−37.963616	−2.275
scheme S′	−37.887068	−0.942	−37.963114	−1.773
EOM-CCSD	−37.883039	3.087	−37.959286	2.055
FCI	−37.886126		−37.961341	

Table 11. Statistical Data for Correlation Gain with Increase in Basis Size

	[(CCT-CCD)/CCD]*100		[(CCQ-CCT)/CCT]*100	
	UGA-SUMRCC(P)	UGA-SUMRCC(S)	UGA-SUMRCC(P)	UGA-SUMRCC(S)
mean	0.1271	0.1274	0.0625	0.0621
SD	0.0198	0.0200	0.0037	0.0045
max gain	0.1456	0.1453	0.0690	0.0690
min gain	0.0779	0.0777	0.0553	0.0532

Though, in an absolute sense, these differences are not very large. The reason may lie in some sort of inadequate description of these states in cc-pVDZ basis. We have also seen that the difference values may be positive or negative, which indicates that both ordinary mean and absolute mean would be necessary to get a feeling of the performance of sufficiency equations vs the full scheme. The signed mean of all the percent difference values is 0.00078%, i.e, a positive number, suggesting that, statistically speaking, the sufficiency results are lower than the full projection scheme. The reason may be attributed to the greater number of degrees of freedom in the sufficiency equations. The percent absolute mean value, an important qualifier for our set of data, is 0.00175%,

Table 14. Singlet and Triplet Excitation Energies (ΔE) of HF in DZV Basis

method	scheme	$^1\Pi$	$^3\Pi$
UGA-QFMRCC	scheme P	0.493533	0.470572
	scheme S	0.492702	0.470053
	scheme P′	0.493850	0.471709
	scheme S′	0.493822	0.471018
UGA-SUMRCC	scheme P	0.493059	0.470113
	scheme S	0.492259	0.469762
	scheme P′	0.493480	0.471374
	scheme S′	0.493386	0.470861
EOM-CCSD		0.482712	0.460635
FCI		0.492826	0.470770

Table 12. Singlet Excitation Energies (ΔE) of H_2O in DZV Basis

method	scheme	$^1B_1$	$^1A_2$	$^1A_1$	$^1B_2$
UGA-QFMRCC	scheme P	0.322132	0.398896	0.409569	0.498643
	scheme S	0.321385	0.397601	0.408268	0.494970
	scheme P′	0.322375	0.397914	0.407658	0.496871
	scheme S′	0.322443	0.398175	0.408680	0.497743
UGA-SUMRCC	scheme P	0.322465	0.399093	0.410051	0.499078
	scheme S	0.321732	0.397893	0.408828	0.495829
	scheme P′	0.322879	0.398271	0.408862	0.497824
	scheme S′	0.322839	0.398530	0.409075	0.498392
EOM-CCSD		0.317842	0.395145	0.405879	0.494547
FCI		0.322704	0.398912	0.410228	0.497564

Table 13. Triplet Excitation Energies (ΔE) of H_2O in DZV Basis

method	scheme	$^3B_1$	$^3A_2$	$^3A_1$	$^3B_2$
UGA-QFMRCC	scheme P	0.293259	0.380042	0.375226	0.449528
	scheme S	0.293661	0.380219	0.375303	0.448740
	scheme P′	0.294848	0.381453	0.375060	0.448941
	scheme S′	0.294947	0.380984	0.375299	0.447629
UGA-SUMRCC	scheme P	0.293501	0.380243	0.375475	0.450457
	scheme S	0.294013	0.380552	0.375911	0.449989
	scheme P′	0.295397	0.381869	0.376116	0.450531
	scheme S′	0.295639	0.381572	0.376610	0.449528
EOM-CCSD		0.289672	0.378106	0.371376	0.446679
FCI		0.294783	0.381390	0.376156	0.450199

certainly not a very large value. The maximum and minimum values and standard deviations of differences are also reasonable quantities (please refer to Table 4). From this analysis, we may conclude that the dispersion of data for sufficiency as against projection is not very wayward.

Our comparison against FCI shows that the full scheme performs pretty well in all cases. Keeping in mind that these are solutions of nonlinear equations, the errors may be both positive and negative. We see that the full scheme gives results mostly above FCI. The sufficiency variant of the parent theory performs somewhat erratically in the sense that it may overshoot or undershoot the FCI values. Though this nature is not observed in the parent theory, when the comparison is done along different states of a particular molecule, the variant using sufficiency is lacking this quality. The absolute percent difference values, on the other hand, in Figure 7 clearly show that they not very large. The primed schemes wherein certain three-body blocks which occur at higher orders of perturbation have been excluded are not quite reliable, indicating that the excluded blocks often play a significant role in the description of excited states.

In the third set of comparisons, we have seen a consistent change in percent correlation with an increase in basis size for our theory (please refer to Table 11). There are no sudden jumps in error as evidenced by the small standard deviation. This is true for both schemes and hence validates our expectation that there are no limitations in the description of excited states for our theory with increasing basis size. The mean and standard deviations are very similar for schemes P and S, indicating that invoking sufficiency does not affect the change of energy with increasing basis size.

Quasi-Fock MRCC. The trends for accuracy as evidenced by difference from FCI values are the same for UGA-QFMRCC and the parent UGA-SUMRCC. Results show a difference on the order of mH. The UGA-QFMRCC predicts excitation energies which are consistently lower than the corresponding value obtained by taking an explicit difference of UGA-SUMRCC excited state energy and CCSD ground state energy (Tables 12−19). Due to the unitary group adapted description of our target state and use of projection equations, higher body G blocks (three and four body) are involved. Thus, although the description of the ground and excited state are well-balanced in terms of operators, there exists a discrepancy at the block level. The use of projection equations necessitates the involvement of certain three and four body blocks which correspond to triples and quadruples as in CCSDtq.[47] These could implicitly contribute to an overcorrelation of the excited state as against the ground state, which is correlated at the purely CCSD level. The more or less consistent improvement over EOM-CCSD is most likely due to the greater incorporation of orbital relaxation.

Table 15. Singlet and Triplet Excitation Energies (ΔE) of BH in cc-pVDZ Basis

method	scheme	$^1\Pi$	$^3\Pi$
UGA-QFMRCC	scheme P	0.107971	0.043900
	scheme S	0.110134	0.046459
	scheme P	0.102949	0.043005
	scheme S′	0.106510	0.043683
UGA-SUMRCC	scheme P	0.109262	0.044440
	scheme S	0.111212	0.046508
	scheme P′	0.105864	0.044158
	scheme S′	0.109831	0.044652
EOM-CCSD		0.111811	0.047337
FCI		0.113699	0.047626

Table 16. Singlet and Triplet Excitation Energies (ΔE) of CH^+ in cc-pVDZ Basis

method	scheme	$^1\Pi$	$^3\Pi$
UGA-QFMRCC	scheme P	0.114014	0.037854
	scheme S	0.114647	0.039080
	scheme P	0.108663	0.036595
	scheme S′	0.112453	0.037271
UGA-SUMRCC	scheme P	0.115143	0.038680
	scheme S	0.115489	0.039613
	scheme P′	0.115489	0.039613
	scheme S′	0.114559	0.038513
EOM-CCSD		0.118588	0.042341
FCI		0.117478	0.042263

Table 17. Singlet Excitation Energies (ΔE) of CH^+ in $14\sigma 5\pi 1\delta$ Basis[a]

method	$^1\Pi$
UGA-QFMRCC (P)	0.115030
CC3	0.119068
STEOM-CC	0.116128
EOM-CCSD	0.119803
FCI	0.118700

[a]Geometry: bond length = 2.13713 au. Ref 48.

Table 19. Singlet and Triplet Excitation Energies (ΔE) of C_2H_2 in aug-cc-pVDZ Basis[a]

method	$1^1\Pi$	$2^1\Pi$	$1^3\Pi$	$2^3\Pi$
UGA-QFMRCC (P)	0.295153	0.309933	0.290207	0.302958
EOM-CCSD	0.304774	0.318854	0.309009	0.314472
experiment	0.299872[b]	0.331109[b]	0.296199	0.314206

[a]Geometry: C(0.000, 0.000, 1.66245), H(0.000, 0.000, 0.60085) in Å. [b]Ref 53.

Table 18. Excitation Energy of H_2O Considering ($1b_1$, $4a_1$, $2b_2$) Orbitals in the Model Space[a]

	$^1B_1$		$^1A_2$		$^3B_1$		$^3A_2$	
method	Sadlej	ANO	Sadlej	ANO	Sadlej	ANO	Sadlej	ANO
UGA-QFMRCC (P)	0.274858	0.277845	0.339898	0.342474	0.258286	0.261563	0.331370	0.334170
EOM-CCSD	0.272035	0.280795	0.336538	0.345359	0.257249	0.266374	0.330241	0.339266
VUMRCC	0.276318				0.264889			
experiment	0.275252[b]		0.334416[c]		0.257245[d]		0.338091[d]	
					0.264595[c]		0.334416[e]	

[a]Geometry: O(0, 0, 0), H(0, ±0.7566, −0.5858) in Å. [b]Ref 49. [c]Ref 50. [d]Ref 51. [e]Ref 52.

6. SUMMARY AND FUTURE OUTLOOK

In this paper, an extensive analysis of several different aspects of UGA-SUMRCC has been undertaken. Detailed proof of size extensivity of the theory for hole−particle model spaces has been presented, using cumulant decomposition of reduced density matrices (RDM). This had not been previously discussed in the earlier paper of ours.[23] A numerical study of the use of a redundant set of linearly dependent excitation operators versus the use of linearly independent combinations of excitation operators has also been undertaken. The former has been found to have mixed performance relative to the latter for the different molecular states studied by us. A systematic study of the performance of the variants of UGA-SUMRCC with increasing basis size showed that no untoward behavior occurs with increasing basis size. An extension of the UGA-SUMRCC for the direct calculation of energy differences has also been developed, along with numerical applications. We have called this method UGA-Quasi-Fock MRCC theory. This has been found to perform satisfactorily. The insight it provides into the nature of excited state physics incorporated into our formulation is significantly enlightening. We find that both the UGA-SUMRCC and UGA-QFMRCC perform satisfactorily, showing a consistent improvement over the popular and widely used EOM-CCSD theory.

Our formulation is well suited for extension to higher valence sectors, which we hope to undertake in the near future to increase the realm of applicability. Like all the effective Hamiltonian formalisms, our theories also suffer from the problem of intruders unless we confine ourselves to the low energy excited states only. However, this difficulty may be bypassed by casting the equations as a dressed CI using an Eigenvalue Independent Partitioning (EIP)/intermediate Hamiltonian technique.[54−58] We hope to work on this too in the near future.

AUTHOR INFORMATION

Corresponding Author

E-mail: pcdm@iacs.res.in.

Notes

The authors declare no competing financial interest.

ACKNOWLEDGMENTS

The authors gratefully acknowledge all the facilities of IACS. D.M. acknowledges the J. C. Bose Fellowship, the Indo-EU MONAMI project, and the Indo-Swedish grant for research support. S.S. thanks the SPM fellowship of the CSIR (India), and A.S. thanks DST for financial support. A.S. and D.M. also thank the IFCPAR/CEFIPRA for generous financial support. It is a pleasure to dedicate this article to Professor Trygve Helgaker on the eve of his 60th birthday. We greet him on this happy occasion and wish him many more years of creative pursuit.

REFERENCES

(1) Čížek, J. *J. Chem. Phys.* **1966**, *45*, 4256−4266.

(2) Bartlett, R. J. Coupled Cluster Theory: An Overview of Recent Developments In *Modern Electronic Structure Theory Part II* ; Yarkony, D. R., Ed.; WS: Singapore, 1999; pp 1047−1131 and references therein.

(3) Coester, F. *Nucl. Phys.* **1958**, *7*, 421−424.

(4) Kummel, H. *Nucl. Phys.* **1960**, *17*, 477−485.

(5) Paldus, J.; Čížek, J.; Shavitt, I. *Phys. Rev. A* **1972**, *5*, 50−67.

(6) Raghavachari, K.; Trucks, G. W.; Pople, J. A.; Head-Gordon, M. *Chem. Phys. Lett.* **1989**, *157*, 479−483.

(7) Shen, J.; Piecuch, P. *P. Chem. Phys.* **2012**, *401*, 180−202.

(8) Li, X.; Peris, G.; Planelles, J.; Rajadell, F.; Paldus, J. *J. Chem. Phys.* **1997**, *107*, 90−98.

(9) Berkovic, S.; Kaldor, U. *J. Chem. Phys.* **1993**, *98*, 3090−3094.

(10) Mukherjee, D.; Moitra, R. K.; Mukhopadhyay, A. *Mol. Phys.* **1977**, *33*, 955−969.

(11) Lindgren, I. *Int. J. Quantum Chem.* **1978**, *S12*, 33−58.

(12) Mukherjee, D.; Moitra, R. K.; Mukhopadhyay, A. *Mol. Phys.* **1975**, *30*, 1861−1888.

(13) Lindgren, I.; Mukherjee, D. *Phys. Rep.* **1987**, *151*, 93−127.

(14) Jeziorski, B.; Monkhorst, H. J. *Phys. Rev.* **1981**, *A24*, 1668−1681.

(15) Jeziorski, B.; Paldus, J. *J. Chem. Phys.* **1988**, *88*, 5673−5687.

(16) Mahapatra, U. S.; Datta, B.; Mukherjee, D. *J. Chem. Phys.* **1999**, *110*, 6171−6188.

(17) Li, X.; Paldus, J. *J. Chem. Phys.* **1994**, *101*, 8812−8826.

(18) Piecuch, P.; Paldus, J. *J. Chem. Phys.* **1994**, *101*, 5875−5890.

(19) Paldus, J.; Piecuch, P.; Pylypow, L.; Jeziorski, B. *Phys. Rev. A* **1993**, *47*, 2738−2782.

(20) Datta, D.; Mukherjee, D. *J. Chem. Phys.* **2009**, *131*, 044124 (1−30).

(21) Datta, D.; Mukherjee, D. *J. Chem. Phys.* **2011**, *134*, 054122 (1−16).

(22) Maitra, R.; Sinha, D.; Mukherjee, D. *J. Chem. Phys.* **2012**, *137*, 024105 (1−24).

(23) Sen, S.; Shee, A.; Mukherjee, D. *J. Chem. Phys.* **2012**, *137*, 074104 (1−17).

(24) Mukherjee, D.; Zaitsevskii, A. *Chem. Phys. Lett.* **1995**, *233*, 605−610.

(25) Sinha, D.; Maitra, R.; Mukherjee, D. *J. Chem. Phys.* **2012**, *137*, 094104 (1−18).

(26) Sekino, H.; Bartlett, R. J. *Int. J. Quantum Chem. Symp.* **1984**, *18*, 255−265.

(27) Geertsen, J.; Rittby, M.; Bartlett, R. J. *Chem. Phys. Lett.* **1989**, *164*, 57−62.

(28) Hirao, K. *J. Chem. Phys.* **1991**, *95*, 3589−3595.

(29) Stanton, J. F.; Bartlett, R. J. *J. Chem. Phys.* **1993**, *98*, 7029−7039.

(30) Nooijen, M.; Bartlett, R. J. *J. Chem. Phys.* **1997**, *106*, 6441−6448.

(31) Nooijen, M.; Bartlett, R. J. *J. Chem. Phys.* **1997**, *106*, 6449−6455.

(32) Nooijen, M.; Bartlett, R. J. *J. Chem. Phys.* **1997**, *107*, 6812−6830.

(33) Jeziorski, B.; Paldus, J.; Jankowski, P. *Int. J. Quantum Chem.* **1995**, *56*, 129−155.

(34) Sinha, D.; Mukhopadhyay, S.; Mukherjee, D. *Chem. Phys. Lett.* **1986**, *129*, 369−374.

(35) Lindgren, I. *Phys. Scr.* **1985**, *32*, 611.

(36) Mukherjee, D. *Chem. Phys. Lett.* **1986**, *125*, 207−212.

(37) Mukherjee, D. *Int. J. Quantum Chem.* **1986**, *S20*, 409−435.

(38) Mukherjee, D. On the Existence and Realization of Size-extensive Effective Hamiltonian Theories for General Model Spaces. In *Condensed Matter Theories*; Arponen, J., Bishop, R. F., Manninen, M., Eds.; Plenum Press: New York, 1988; 3.

(39) Mukhopadhyay, D.; Mukherjee, D. *Chem. Phys. Lett.* **1989**, *163*, 171−177.

(40) In our parent UGA-SUMRCC paper,[23] we commented on the simplification of the Bloch Equation for 1h−1p IMS, as studied in ref 34 using VUMRCC. We want to emphasize that such simplifications are not valid in the UGA-SUMRCC, though for the 1h−1p situation the necessary modifications are very minor and have been incorporated both in our parent paper[23] and in this paper.

(41) Jana, D.; Datta, D.; Mukherjee, D. *Chem. Phys.* **2006**, *329*, 290−306.

(42) Paldus, J.; Li, X. Unitary Group Approach Valence Bond and Coupled Cluster Method. In *Symmetries in Science VI: From the Rotation Group to Quantum Algebra*; Gruber, B., Ed.; Plenum: New York, 1993; pp 573−591.

(43) Paldus, J.; Li, X. *Int. J. Quantum Chem. Symp.* **1993**, *27*, 269−285.

(44) Kutzelnigg, W.; Mukherjee, D. *J. Chem. Phys.* **1999**, *110*, 2800−2809.

(45) GAMESS. *J. Comput. Chem.* **1993**, *14*, 1347−1363.

(46) DALTON, release 2.0(2005), a molecular electronic structure program. See http//www.kjemi.uio.no/software/dalton/dalton.html (accessed April 2013).
(47) Piecuch, P.; Kucharski, S. A.; Bartlett, R. J. *J. Chem. Phys.* **1999**, *110*, 6103−6122.
(48) Olsen, J.; Sanchez De Meras, A.; Jensen, H. J. A.; Jorgensen, P. *Chem. Phys. Lett.* **1989**, *154*, 380−386.
(49) Johns, J. W. C. *Can. J. Phys.* **1963**, *41*, 209−215.
(50) Chutjian, A.; Trajmer, S.; Hall, R. I. *J. Chem. Phys.* **1975**, *63*, 892−898.
(51) Knoop, W. E.; Brongersma, H. H.; Oosterhoff, C. J. *Chem. Phys. Lett.* **1972**, *13*, 20−23.
(52) Schulz, G. *J. Chem. Phys.* **1960**, *33*, 1661−1665.
(53) Malsch, K.; Rebentisch, R.; Swiderek, P.; Hohlneicher, G. *Theor. Chem. Acc.* **1998**, *100*, 171−182.
(54) Mukhopadhyay, D.; Datta, B.; Mukherjee, D. *Chem. Phys. Lett.* **1992**, *197*, 236−242.
(55) Musial, M.; Bartlett, R. J. *J. Chem. Phys.* **2008**, *129*, 244111 (1−6).
(56) Sinha, D.; Mukhopadhyay, S. K.; Chaudhuri, R.; Mukherjee, D. *Chem. Phys. Lett.* **1989**, *154*, 544−549.
(57) Chaudhuri, R.; Mukhopadhyay, D.; Mukherjee, D. *Chem. Phys. Lett.* **1989**, *162*, 393−398.
(58) Datta, B.; Chaudhuri, R.; Mukherjee, D. *J. Mol. Struct. (THEOCHEM)* **1996**, *361*, 21−31.